A theoretical framework for interpretation and prediction of magneto-optical measurements

Viktor Frilén

Supervisors: Oscar Grånäs and Mohamed Elhanoty

Subject reader: Anders Bergman

July 26, 2023

UPPSALA
UNIVERSITET

Abstract

The interplay of experiments and theory is essential to deepen our understanding of magnetization dynamics. This thesis aims to serve as a bridge between these two aspects by establishing a mathematical framework that enables the computation of optical observable quantities based on theoretical models. The equations are cast in a matrix representation that is well-suited for performing numerical simulations. Additionally, the generality of these methods enables their application to layered media with any geometry, regardless of whether they possess magnetic properties or not. Furthermore, it explores the various perspectives and physical mechanisms involved in magneto-optic measurements to provide the reader with a self consistent introduction to the subject matter. Numerical calculations are presented for bulk Fe, alternating layers of Fe/Au and Ni with a MgO coating and a SiO substrate for different energies, angle of incident and magnetization direction. The results demonstrate the effectiveness of the method in predicting measurable outcomes from theoretical considerations and enables the analysis of optimal experimental configurations.

Sammanfattning

Samverkan mellan experiment och teori är avgörande för fördjupa vår förståelse av magnetiska system och deras dynamik. Målet med denna uppsats är att etablera en koppling mellan dessa två aspekter genom att formulera ett matematiskt ramverk som möjliggör beräkningar av optiska observerbara storheter baserat på teoretiska modeller. Ekvationerna formuleras med matriser vilket är väl lämpat för att utföra numeriska simuleringar. Dessutom möjliggör metodens generella natur tillämpning på skiktade material av godtycklig geometri, oavsett om de har magnetiska egenskaper eller inte. Vidare utforskar uppsatsen olika perspektiv och fysikaliska mekanismer som är involverade i magneto-optiska mätningar för att ge läsaren en självständig introduktion till ämnet. Numeriska beräkningar presenteras för bulkjärn, växlande lager av Fe/Au och Ni med en MgO-beläggning och ett SiO-substrat för olika energier, infallsvinkel och magnetiseringsriktning. Resultaten visar på metodens förmåga att förutsäga mätbara resultat baserat på teoretiska överväganden och tillåter analys av optimala experimentella uppställningar.

Contents

1 Introduction

Today we as a species face large problems that threaten our very existence. One of the most eminent is the approaching threat of climate change that already shows its presence in various places around the world. We as humans have to collaborate and come up with solutions in order to avoid the possibly catastrophic not so distant future. The best solution as I see it is for us to change our lifestyles and live sustainably, far from our capitalistic past of consumerism. Since this option seems impossible in our current political climate and conflict driven world, we might have to rely more on the second option which is technology. The technological progress is constantly accelerating with an increasing research focus on alternative green energy sources, new sustainable materials and more energy efficient devices.

With the increasing number of people having access to modern technologies that is also becoming progressively more advanced, the need for efficient solutions is crucial in order to fulfill the climate goals set in the Paris agreements. As an example, the internet is estimated to use 20% of our energy consumption in 2030 [1]. How we store, process and transfer data is encompassed in the broad term information technology, which is one of the important issues we are facing today. As the parts of our devices gets smaller to handle an increasing number of computations, we are approaching a dead end in conventional electronics. Heat generation disturbs the signal and put a lower bound on the size of conventional transistors, which is the base of all electronics.

One of the most promising solution to this problem is what is called spintronics. As the name suggests spintronics uses not only charge as carried of information as conventional electronics, but also incorporate the electrons spin degrees of freedom which increases the information density. The possibility of pure spin currents without any charge transfer and thus without any heat generation would be the ideal scenario for circuits. Because of the potential possibilities, spintronics has inspired significant research efforts in the last years and field is rapidly developing[2][3][4].

Beside spin currents to revolutionize circuits and transistor technologies, spintronics also encompasses data storing, which goes back to the internet as one of the major energy consuming sectors. Much of the data stored in data centers and large scale IT facilities is on mechanical hard drives[5]. The information in the light signal transmitted through optical fibers needs to be converted and physically imprinted on the hard drives and in this process energy is lost and the efficiency is low. An ideal situation would be to imprint information directly by optically inducing magnetization onto the hard drives. Because high spacial resolution of today's lasers, information could in principle be store in microscopically sized domains in the material which then also could be read with lasers.

The road to commercial spin based technologies although promising, is paved with obstacles that we need to overcome. These are problems concerning injection, manipulation, transport and detection of spin. One of the major ones is

the required low temperatures in order to ensure stability and room temperature spintronics would be the ultimate goal. To succeed in these challenges, better techniques needs to be developed, new materials designed and the underlying mechanisms better understood.

Because of the many elements available, there is an almost infinite number of combinations possible when designing a compound, making simple trial and error approach cumbersome and inefficient. Here first principles calculations serve as a powerful tool in predicting material properties. Furthermore, they are invaluable for understanding the underlying mechanisms and the dominant processes. To then compare with experiments, the calculated microscopic observables needs to be related to macroscopic quantities.

This thesis focus is on the bridge between theory and experiment. More specifically it investigate the effects on light as it propagates through a magnetic medium (magneto-optical effects) both micro- and macroscopically. It investigates the different contributions from a quantum mechanical perspective and how these can be related to elements in the dielectric tensor which enters Maxwell's equations. The main part is devoted to the development of (a mathematical framework in the form of) a matrix calculus based on Maxwell's equations in order to solve optical problems of arbitrary geometry. Optical quantities is derived for a general experimental setup in which the dielectric tensor plays the role of a bridge between the microscopic and macroscopic description.

The calculus is then used to investigate experimental setups and to present optimal chose of parameters such as angle of incidence, magnetization direction and frequency of light, to maximize the signal. Calculations are carried our for the ferromagnetic elements Cobolt, Nickel and Iron, with their dielectric functions given from (time dependent) density function theory (TD)DFT.

2 Review/Background

The way light interacts with magnetic matter is an extensive and multifaceted subject, thereby allowing for a plethora of approaches and perspectives to be considered. While it is not possible to encompass all aspects of the problem at hand, this thesis endeavors to address the most essential components required to ensure self-consistency. The primary focus is on classical optics, with Sections (maxwells equations, waves, optics and matrix method) serving as the critical sections for comprehending the results. Other sections may be skipped or read to gain a background understanding of the underlying principles governing the phenomena and the methods used for first principle calculations.

The review is structured as follows. First, Maxwell's equations which describe the behavior of the electric and magnetic field will be explained and how light waves are a solution to these equations. Then an explanation of the theory of classical optics will be provided, including a discussion of the assumptions and approximations required for its macroscopic treatment of light. The subsequent sections will then cover the quantum mechanical treatment of magnetism and its effects on the propagation of light. Two microscopical models

will be presented, along with their relation to the theory of optics through the dielectric function. Additionally, density functional theory, which plays a vital role in proper treatment of materials and enables first-principle calculations of many interacting particles, will be briefly explained. With a sound theoretical basis established, a matrix calculus will be derived for solving complex optical problems involving multiple reflections and refractions in magnetic materials. This matrix formulation will be the primary tool used in deriving the results presented in the results section.

2.1 Maxwell's equations

Maxwell's equations (1-2) form the foundation of classical electrodynamics. These equations describes the dynamical interplay between the electric field $\mathbf{E}$ and the magnetic field $\mathbf{B}$ aswell as how these fields are created by and interacts with charges ρ and currents $\mathbf{J}$. The macroscopic treatment of light, which is the focus of this thesis, is built upon these four differential equations and it will later be shown how quantum mechanical considerations can be included. The equations in Gaussian units are written as

$$\boldsymbol{\nabla} \cdot \mathbf{D} = 4\pi\rho, \qquad \boldsymbol{\nabla} \times \mathbf{E} = -\frac{1}{c}\frac{\partial \mathbf{B}}{\partial t}, \tag{1}$$

$$\boldsymbol{\nabla} \cdot \mathbf{B} = 0, \qquad \boldsymbol{\nabla} \times \mathbf{H} = \frac{4\pi}{c}\mathbf{J} + \frac{1}{c}\frac{\partial \mathbf{D}}{\partial t}, \tag{2}$$

with

$$\mathbf{D} = \mathbf{E} + 4\pi\mathbf{P}, \tag{3}$$

$$\mathbf{B} = \mathbf{H} + 4\pi\mathbf{M}. \tag{4}$$

The polarization field $\mathbf{P}$ and the magnetization field $\mathbf{M}$ describe the response from a material and are the results of the rearrangement of a charges due to an external fields $\mathbf{D}$ or $\mathbf{H}$. The actual physical field is always given by $\mathbf{E}$ and $\mathbf{B}$. In vacuum where there are no charges nor currents, $\mathbf{P}$ and $\mathbf{M}$ are zero. Maxwell's equations can be solved as a boundary value problem with the boundary conditions

$$\hat{\mathbf{n}} \cdot (\mathbf{D_2} - \mathbf{D_1}) = 4\pi\sigma_{surface}, \qquad \hat{\mathbf{n}} \times (\mathbf{E_2} - \mathbf{E_1}) = 0, \tag{5}$$

$$\hat{\mathbf{n}} \cdot (\mathbf{B_2} - \mathbf{B_1}) = 0, \qquad \hat{\mathbf{n}} \times (\mathbf{H_2} - \mathbf{H_1}) = 4\pi\mathbf{J}_{surface}, \tag{6}$$

which follows from the Equations (1-2). If there is no free charge nor free current at the surface then

$$\hat{\mathbf{n}} \cdot (\mathbf{D_2} - \mathbf{D_1}) = 0, \qquad \hat{\mathbf{n}} \times (\mathbf{E_2} - \mathbf{E_1}) = 0, \tag{7}$$

$$\hat{\mathbf{n}} \cdot (\mathbf{B_2} - \mathbf{B_1}) = 0, \qquad \hat{\mathbf{n}} \times (\mathbf{H_2} - \mathbf{H_1}) = 0. \tag{8}$$

This shows that the parallel component of the $\mathbf{E}$-field and the $\mathbf{H}$-field is continuous across the surface[6]. These boundary conditions will be used when looking

at reflection and refraction of light. If one assumes a linear response then

$$\mathbf{D} = \epsilon \mathbf{E}, \tag{9}$$

$$\mathbf{B} = \mu \mathbf{H}, \tag{10}$$

$$\mathbf{J} = \sigma \mathbf{E}, \tag{11}$$

and in vacuum, $\epsilon = \mu = 1$ and $\sigma = 0$. For the simple case of isotropic media ϵ, μ and σ are scalars, but they are generally represented by 3×3-matrices.

The permeability μ is often very close to 1 and $\mu = 1$ will sometimes be assumed in this thesis because of the photon energies of interest and an argument for this is explained in Section 2.3. When the dielectric function ϵ is assumed to be complex, it becomes a function of the conductivity σ and one can be calculated from the other. Hence it is often enough to do the calculations and derivations from ϵ, which is the one mentioned most often in this text.

If one assumes no free charges, $\boldsymbol{\nabla} \cdot \mathbf{D} = 0$ and Maxwell's equations becomes

$$\boldsymbol{\nabla} \cdot \mathbf{D} = 0 \qquad \boldsymbol{\nabla} \times \mathbf{E} = -\frac{1}{c}\frac{\partial \mathbf{B}}{\partial t} \tag{12}$$

$$\boldsymbol{\nabla} \cdot \mathbf{B} = 0 \qquad \boldsymbol{\nabla} \times \mathbf{H} = \frac{4\pi}{c}\sigma \mathbf{E} + \epsilon \frac{1}{c}\frac{\partial \mathbf{E}}{\partial t} \tag{13}$$

The last equation can be written as

$$\boldsymbol{\nabla} \times \mathbf{H} = \frac{1}{c}\frac{\partial \mathbf{D}}{\partial t} \tag{14}$$

if one keeps in mind that ϵ is allowed to be complex.

It is through the dielectric function ϵ and the magnetic permeability μ that a microscopic theory can be compared with optical experiments. These microscopic models vary in sophistication and in Section 2.5.1 a simple semi-classical model will be used to derive ϵ and in Section 2.8.1 a quantum mechanical approach is explained. For the results presented in Section 5, the dielectric function was calculated from linear response density functional theory.

Maxwell's equations in gaussian units (assume $\mu = 1$):

$$\boldsymbol{\nabla} \cdot \mathbf{D} = 0 \qquad \boldsymbol{\nabla} \times \mathbf{E} = -\frac{1}{c}\frac{\partial \mathbf{B}}{\partial t} \tag{15}$$

$$\boldsymbol{\nabla} \cdot \mathbf{H} = 0 \qquad \boldsymbol{\nabla} \times \mathbf{H} = \frac{1}{c}\frac{\partial \mathbf{D}}{\partial t} \tag{16}$$

2.2 Light as waves or plane waves solution to Maxwell's equations

The pinnacle of the work done by James Clerk Maxwell, Micheal Faraday and many others in the 19th century was the interpretation of light in terms of electromagnetic waves with the property of a finite propagation velocity. The wave equation follows easily from Maxwell's equations by using the vector relation

$$\boldsymbol{\nabla} \times (\boldsymbol{\nabla} \times \mathbf{A}) = \boldsymbol{\nabla}(\boldsymbol{\nabla} \cdot \mathbf{A}) - \boldsymbol{\nabla}^{\mathbf{2}}\mathbf{A}. \tag{17}$$

In vacuum ($\boldsymbol{\nabla} \cdot \mathbf{E} = 0$, $\mathbf{J} = 0$) one get the equation

$$\nabla^2 \mathbf{E} = \frac{1}{c^2} \frac{\partial^2}{\partial t^2} \mathbf{E}. \tag{18}$$

In one dimension $\nabla^2 \to \frac{\partial^2}{\partial x^2}$, and it's simple to show that functions of the form $f = f(x \pm ct)$ solves this equation

$$\frac{\partial^2}{\partial x^2} f(x \pm ct) = f'' = \frac{1}{c^2} \frac{\partial^2}{\partial t^2} f(x \pm ct) = \frac{1}{c^2} (\pm c)^2 f'' = f''. \tag{19}$$

What this tells us is that the function at a position x_1 and time t_1 is related to what the function looked at another position x_0 at time t_0. With $t_0 = 0$ the relation becomes $f(x_1 - ct_1) = f(x_0)$ or $x_1 - x_0 = \Delta x = ct_1$. c is then easily interpreted as the speed of propagation. This is the defining characteristic of a wave and why this equation is called the wave equation.

When working with waves it's convenient to represent them using the complex exponential function $e^{ik(x-ct)} = \cos(k(x-ct)) + i \sin(k(x-ct))$ since $d(e^f) = f' e^f$.

In matter, with the linear approximation (Equations (12-13) the wave equations has an extra term due to the induced current[7]

$$\nabla^2 \mathbf{E} = \frac{\epsilon \mu}{c^2} \frac{\partial^2 \mathbf{E}}{\partial t^2} + \frac{4\pi\sigma\mu}{c^2} \frac{\partial \mathbf{E}}{\partial t}, \tag{20}$$

$$\nabla^2 \mathbf{H} = \frac{\epsilon \mu}{c^2} \frac{\partial^2 \mathbf{H}}{\partial t^2} + \frac{4\pi\sigma\mu}{c^2} \frac{\partial \mathbf{H}}{\partial t}. \tag{21}$$

By substituting the plane wave solution

$$\mathbf{E} = \mathbf{E}_0 e^{i(\mathbf{K} \cdot \mathbf{r} - \omega t)}, \tag{22}$$

$$\mathbf{H} = \mathbf{H}_0 e^{i(\mathbf{K} \cdot \mathbf{r} - \omega t)}, \tag{23}$$

into the wave equation yields, one gets

$$K^2 = \frac{\omega^2}{c^2} \mu (\epsilon + i 4\pi \frac{\sigma}{\omega}), \tag{24}$$

$$\epsilon_{complex} = \epsilon + i 4\pi \frac{\sigma}{\omega} = \epsilon_1 + i\epsilon_2. \tag{25}$$

With the induced current, the wave number K naturally becomes complex and the relation $k = \frac{\omega}{c} n$ for the refractive index can then be generalized to $K = \frac{\omega}{c} N$. Then we have the following useful relations

$$K = \frac{\omega}{c} N = k + i\kappa, \tag{26}$$

$$N^2 = \mu \epsilon_{complex}. \tag{27}$$

The complex index of refraction is often written as

$$N = n + ik, \tag{28}$$

where n is the index of refraction and k the attenuation coefficient. Here there is an unfortunate instance of using the same notation to represent the real part of K and imaginary part of N, but often only N is used and K is rewritten with Equation (26).

By substituting the expression for N in the plane wave ansatz (22), in 1D one gets

$$\mathbf{E}_0 e^{i\frac{\omega}{c}(Nx-ct)} = \mathbf{E}_0 e^{i\frac{\omega}{c}(nx-ct)} e^{-\frac{\omega}{c}kx}. \tag{29}$$

The attenuation coefficient causes the wave to exponentially decay as a function of x because the wave looses its energy to the charges in the material.

2.3 $\mu = 1$ assumption

When studying light in the optical regime, $\mu = 1$ is often assumed. Here an argument for this assumption will be presented based on the one done by L.D Landau and E. M. Lifshitz [8]. The relation between the $\mathbf{H}$ and $\mathbf{B}$ field is

$$\mathbf{B} = \mathbf{H} + 4\pi\mathbf{M}, \tag{30}$$

which for weak fields can be written as

$$\mathbf{B} = (1 + 4\pi\chi)\mathbf{H} = \mu\mathbf{H}. \tag{31}$$

The interpretation of the magnetization vector $\mathbf{M}$ comes from the Maxwell equation in the static case ($\frac{\partial}{\partial t} = 0$)

$$\boldsymbol{\nabla} \times \mathbf{B} = \frac{4\pi}{c}\mathbf{j}. \tag{32}$$

The current density $\mathbf{j}$ is zero in vacuum but doesn't have to be in a media. But if one assume that for an arbitrary cross-section of the medium, there is no net-current:

$$\int \mathbf{j} \cdot d\mathbf{a} = 0. \tag{33}$$

Then the current density can be written as

$$\mathbf{j} = c\boldsymbol{\nabla} \times \mathbf{M} \tag{34}$$

and thus

$$\boldsymbol{\nabla} \times \mathbf{B} = 4\pi\boldsymbol{\nabla} \times \mathbf{M}, \tag{35}$$

$$\boldsymbol{\nabla} \times \mathbf{H} = 0, \tag{36}$$

$$\mathbf{H} = \mathbf{B} - 4\pi\mathbf{M}. \tag{37}$$

The magnetic moment has the general form

$$\boldsymbol{\tau} = \frac{1}{2c}\int \mathbf{r} \times \mathbf{j}\, dV = \frac{1}{2}\int \mathbf{r} \times (\boldsymbol{\nabla} \times \mathbf{M})\, dV. \tag{38}$$

Here volume V is arbitrary, as long as it contains the object, since $\mathbf{j} = 0$ and $\mathbf{M} = 0$ outside the object. With the help of product rules, the integral can be written as

$$\int \mathbf{r} \times (\boldsymbol{\nabla} \times \mathbf{M})\, dV = -\oint \mathbf{r} \times (\mathbf{M} \times d\mathbf{a}) - \int (\mathbf{M} \times \boldsymbol{\nabla}) \times \mathbf{r}\, dV. \tag{39}$$

The first surface integral is zero since $\mathbf{M} = 0$ outside the object. The second integrand is

$$(\mathbf{M} \times \boldsymbol{\nabla}) \times \mathbf{r} = -\mathbf{M}\boldsymbol{\nabla} \cdot \mathbf{r} + \mathbf{M} = -2\mathbf{M}, \tag{40}$$

and the final result becomes

$$\boldsymbol{\tau} = \int \mathbf{M}\, dV. \tag{41}$$

The interpretation of $\mathbf{M}$ is then the magnetization per volume. This physical meaning given to $\mathbf{M}$ followed from the assumption that $\mathbf{j} = c\boldsymbol{\nabla} \times \mathbf{M}$. In the non-static case

$$\boldsymbol{\nabla} \times \mathbf{H} = \frac{1}{c}\frac{\partial \mathbf{D}}{\partial t}, \tag{42}$$

$$\boldsymbol{\nabla} \times \mathbf{B} = \frac{4\pi}{c}\mathbf{j} + \frac{1}{c}\frac{\partial \mathbf{E}}{\partial t}, \tag{43}$$

and the current density is instead

$$\mathbf{j} = c\boldsymbol{\nabla} \times \mathbf{M} + \frac{\partial \mathbf{P}}{\partial t}. \tag{44}$$

So for $\mathbf{M}$ and therefore the magnetic susceptibility χ to have any physical meaning, $\frac{\partial \mathbf{P}}{\partial t}$ needs to be much smaller than $c\boldsymbol{\nabla} \times \mathbf{M}$. Then the polarization term can be neglected and the result in Equation (41) is still valid.

To see why this is not the case for optical frequencies, one can do some estimates. $c\boldsymbol{\nabla} \times \mathbf{M} \sim \frac{cM}{l}$ with l being a length dimension of the object. This term is thus largest for small bodies. $\frac{\partial \mathbf{P}}{\partial t}$ is small for weak $\mathbf{E}$-fields, but since $E \sim H$ for electromagnetic waves, this estimate will not help. Instead imagine placing the object in a changing magnetic field, and that $\mathbf{E}$ comes from induction. Then $\boldsymbol{\nabla} \times \mathbf{E} = -\frac{1}{c}\frac{\partial \mathbf{B}}{\partial t}$, hence $\frac{E}{l} \sim \frac{\omega}{c}H$, or $E \sim \frac{l\omega}{c}H$. The polarization $\mathbf{P} = \frac{1}{4\pi}(\epsilon - 1)\mathbf{E} \sim E$, with the assumption that $\frac{1}{4\pi}(\epsilon - 1) \sim 1$. Then $\frac{\partial \mathbf{P}}{\partial t} \sim \omega E \sim \frac{l\omega^2}{c}H$. For the magnetization vector $\mathbf{M} = \chi\mathbf{H}$, $c\boldsymbol{\nabla} \times \mathbf{M} \sim \frac{c\chi}{l}H$. So the estimate for the condition $\frac{\partial \mathbf{P}}{\partial t} \ll c\boldsymbol{\nabla} \times \mathbf{M}$ is $\frac{\omega^2 l}{c}H \ll \frac{c\chi}{l}H$ or

$$l^2 \ll \frac{c^2\chi}{\omega^2}. \tag{45}$$

The dimensions of the object should be macroscopic, hence $l \gg a$, where a is an atomic dimension. For optical frequencies $\omega = \frac{c}{\lambda} \sim \frac{v}{a}$, where v is the velocity of the electron. For a non-ferromagnetic body, the magnetization is a relativistic

effect and $\chi \sim \frac{v^2}{c^2}$. $\frac{v}{c}$ shows up ones in the interaction with the magnetic field and ones in the magnetic moments of the atoms. The inequality that needs to be fulfilled for the susceptibility to be physically meaningful is

$$l^2 \ll a^2. \tag{46}$$

Thus there is no meaning in using the magnetic susceptibility in the optical frequency range and people set $\mu = 1$ and distinguishing between the B- and H-field is excessive [8].

2.4 Classical optics

The macroscopic Maxwell theory of optics used throughout this text is based on the fact that optical experiments with monochromatic light have a spacial resolution on the order of wavelengths. Hence volumes that are small compared to the wavelength of light still contains many atoms. An example is in the experiment in Ref. [9] where a 633 nm $= 6.33 \times 10^{-7}$ m laser is used. The atomic spacing in a material is in order of Ångstöm, 1 Å $= 10^{-10}$ m. A small volume compared to the laser would still contain thousands of atoms. The theory averages over small volumes and thus smooth out any microscopic fluctuations. These approximately continuous optical media can be assigned a refractive index and an attenuation coefficient which describes how the light bends when entering a media and how much of the light that gets absorbed while propagating through it [10]. Together these two form the complex index of refraction. There are materials which can be assigned a single refraction index, but this is generally not the case. With the refractive index and the boundary conditions from Maxwell's equations, reflection and transmission at medium boundaries can be calculated.

2.4.1 Classification of optical media

All media can be divided into single refracting and double refracting. Double refracting media can be further classified by whether they are isotropic or anisotropic, uniaxial or biaxial and if they are optically active or not. What is common to double refracting media is for a given direction and frequency, there are just two polarizations for which have a definite refractive index. This is a requirement for a definite wavelength and propagation velocity. These two polarizations are in general elliptical, with same eccentricity and major axes at right angles. One of them are right circular polarized (RCP) and the other is left circular polarized (LCP). The general plane wave is then a superposition of these two polarizations [10].

For a non-active media to be double refracting, it has to be anisotropic. The two polarizations for any given direction of propagation are linear and at right angles and the index of refraction varies across different directions. In the

principle system, the index of refraction can be written as

$$n = \begin{pmatrix} n_x & 0 & 0 \\ 0 & n_y & 0 \\ 0 & 0 & n_z \end{pmatrix}, \tag{47}$$

here the diagonal elements are called the principal index of refraction. For uniaxial media, two of the three principles indices are the same, e.g: $n_x = n_y = n_o$, $n_z = n_e$. Then the z-axis is called the optical axis, since a waye propagating along this direction will experience a single refraction index n_o. n_o is called the ordinary refractive index and n_e is called the extra ordinary refractive index. If all three indices are different, the media is called biaxial.

Another term that is used in optics is dichroism. This is when the material is absorbing, with different attenuation depending on the polarization. This can be understood microscopically by materials having different resonance frequencies depending on the atoms and geometry of the crystal.

Optical activity is when the polarization direction is rotated by a non-magnetic sample. This is often associated with a certain handedness, or chirality, of the charge distribution. An example is SiO_2, which crystal structure is in a corkscrew arrangement which causes LCP and RCP to have different refractive indexes.

Magneto-optical rotation on the other hand is a rotation of the polarization direction in the presence of a magnetic field or alignment of magnetic moments, which breaks time-reversal symmetry which gives the sample a sense of handiness in time [11]. This gives the medium different refractive indices for RCP and LCP and the effect is interesting when doing measurements on magnetic materials and will be studied further in thesis.

2.5 Magneto-optic effects

The interaction between light and matter is influenced by the magnetic state of the medium and depends on the electronic structure of the material. This interaction gives rise to phenomena known as magneto-optic effects, which occur when electromagnetic radiation interacts with magnetically polarized materials.

When light is incident on a magnetic material, the state of polarization changes and this can effectively be introduced through off-diagonal elements in the dielectric function (Equation (9)). The polarization changes both for the reflected and transmitted light and the effect is then called magneto-optic Kerr effect (MOKE) or Faraday rotation respectively. A third possible measurement is to look how the light is absorbed in the material, magnetic dichroism. Depending on the situation all of these effects can be measured, but when doing measurements on metals, which naturally have high absorption, it is often more convenient to measure the polarization of the reflected wave (MOKE).

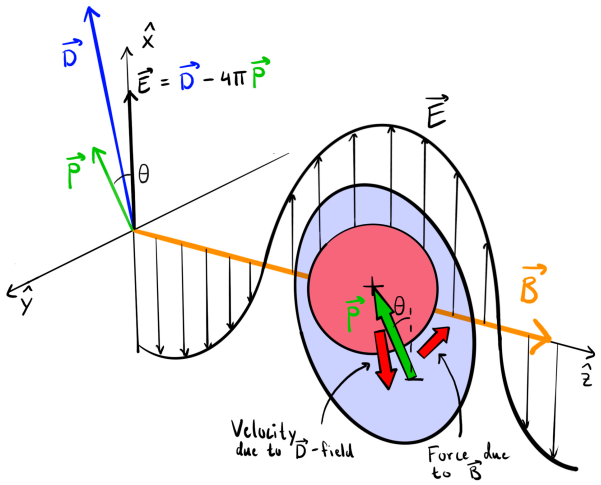

Figure 1: A classical model on how the polarization and thus the electrical field gets rotated in a material when a magnetic field is present.

How magnetism affect the polarization by rotation is illustrated classically in Figure 1. Here the external D-field causes the electron density to move in the opposite direction, but because of the B-field and the Lorentz force $\mathbf{F} = q(\mathbf{v} \times \mathbf{B})$, the electron density will also start to move perpendicular to the D-field. These vectors are written in the x-y-plane which make it clear that the external field D gets rotated to E by the material. The dielectric function for a magnetic material magnetized in the z-direction with cubic symmetry can be written as

$$\epsilon = \begin{pmatrix} \epsilon_{xx} & \epsilon_{xy} & 0 \\ -\epsilon_{xy} & \epsilon_{xx} & 0 \\ 0 & 0 & \epsilon_{zz} \end{pmatrix}, \tag{48}$$

and for an E-field in the x-direction

$$\mathbf{D} = \epsilon \begin{pmatrix} E_x \\ 0 \\ 0 \end{pmatrix} = \begin{pmatrix} \epsilon_{xx} E_x \\ -\epsilon_{xy} E_x \\ 0 \end{pmatrix} \tag{49}$$

When the dielectric function is calculated from the same model below, it is seen that $\epsilon_{xx} > 0$ and $\epsilon_{xy} < 0$ (Equations (63-65) and (68)), hence the D-field in Equation (49) points in the same direction as in Figure 1. This example is just to give an intuition on the fields interact and why the polarization is rotated when magnetism enters the picture, but the actual situation is of course much more complicated.

For experiments in the optical region, the general procedure is to shine linearly or circular polarized light onto a sample and then to measure what is

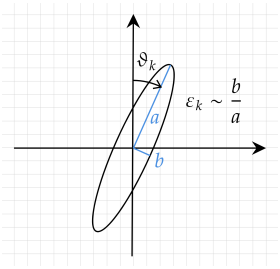

Figure 2: The change of polarization due to MOKE, called complex Kerr rotation.

called the complex Kerr rotation[12]

$$\vartheta_k = \theta_k + i\epsilon_k, \tag{50}$$

which for p- respectively s-polarized light are

$$\vartheta_k^p = \frac{r_{sp}}{r_{pp}}, \qquad \vartheta_k^s = \frac{r_{ps}}{r_{ss}}, \tag{51}$$

This describes a rotation and change in eccentricity of the ellipse of polarization in the reflected light as illustrated in Figure 2. The incoming light is either linear polarized, which is in a superposition of LCP and RPC, or circular polarized. Because the magnetic field (or the effective magnetic field from the alignment of spins), time-reversal symmetry is broken causing LCP and RCP light to have different index of refraction ($N = n + ik$), which both leads to a difference in absorption due to k and phase due to n, hence a change in eccentricity and a rotation of the ellipse of polarization.

The r_{ij} is the reflection coefficients in the Fresnel reflection matrix

$$\begin{pmatrix} E_{sr} \\ E_{pr} \end{pmatrix} = \begin{pmatrix} r_{ss} & r_{sp} \\ r_{ps} & r_{pp} \end{pmatrix} \begin{pmatrix} E_{si} \\ E_{pi} \end{pmatrix}, \tag{52}$$

which say how much of the incident s/p-polarized light that is reflected as s/p-polarized. How to calculate this matrix and a similar one for transmission is described in Section 3 and is the main part of this thesis. Other quantities than the complex Kerr rotation can also measured, e.g for light in the XUV region ($\sim$ 10-124 eV) it is common to measure the asymmetry parameter (Equation (252)) but this quantity is also a function of the reflection coefficients.

2.5.1 Lorentz model of an oscillating electron

The refractive index and attenuation coefficient together form the complex index of refraction. This can be derived from different microscopic models, often through a linear response theory. Here a simple model called the Lorentz oscillator model will be used to derive the optical response and to illustrate how a

microscopic model can be used in deriving the complex refractive index. With the addition of a magnetic field in the z-direction, the derivation, inspired by K. Sato and T. Ishibashi [13], will also show how magnetism introduced off-diagonal elements in the dielectric function.

In this crude model, the electron is thought of as a classical object, bound to the stationary nuclei through a restoring force $m\omega_0^2\mathbf{r}$. The electron also experience a dampening force $m\gamma\frac{\partial\mathbf{r}}{\partial t}$, that depends on the speed, since at higher speeds, there are more collisions. The equation of motion can then be written as

$$m\frac{\partial^2\mathbf{r}}{\partial t^2} + m\gamma\frac{\partial\mathbf{r}}{\partial t} + m\omega_0^2\mathbf{r} + e\left(\mathbf{E}(t) + \frac{\partial\mathbf{r}}{\partial t}\times\mathbf{B}\right) = 0. \tag{53}$$

Here $\gamma = \frac{1}{\tau}$ is the dampening factor, ω_0 is the resonance frequency of the system, m is the mass of the electron and $-e\mathbf{E}(t)$ is the driving force from the electric field. The last term represent the Lorentz force with a constant magnetic field. By assuming plane waves and doing a simple ansatz for $\mathbf{r}$

$$\mathbf{E} = \mathbf{E}_0 e^{-i\omega t}, \tag{54}$$
$$\mathbf{r} = \mathbf{r}_0 e^{-i\omega t}, \tag{55}$$
$$\mathbf{B} = (0, 0, B), \tag{56}$$

gives

$$m(\omega_0^2 - \omega^2 - i\omega\gamma)r_{0x} + iq\omega B r_y = qE_{0x}, \tag{57}$$
$$m(\omega_0^2 - \omega^2 - i\omega\gamma)r_{0y} - iq\omega B r_y = qE_{0y}, \tag{58}$$
$$m(\omega_0^2 - \omega^2 - i\omega\gamma)r_{0z} = qE_{0z}. \tag{59}$$
$$\tag{60}$$

This equation can be solved for $\mathbf{r} = \hat{\alpha}(\omega)\mathbf{E}$. From the definition of an electric dipole $\mathbf{p} = -e\mathbf{r}$ and with the atomic density N, one gets the following expression for the macroscopic polarization

$$\mathbf{P} = N\mathbf{p} = -Ne\hat{\alpha}\mathbf{E} = \epsilon_0\chi\mathbf{E}, \tag{61}$$

with

$$\chi = \begin{pmatrix} \chi_{xx} & \chi_{xy} & 0 \\ -\chi_{xy} & \chi_{xx} & 0 \\ 0 & 0 & \chi_{zz} \end{pmatrix}, \tag{62}$$

and

$$\chi_{xx} = -\frac{Ne^2}{m\epsilon_0}\frac{\omega^2 + i\gamma\omega - \omega_0^2}{(\omega^2 + i\gamma\omega - \omega_0^2)^2 - \omega_c^2\omega^2}, \tag{63}$$
$$\chi_{xy} = -\frac{Ne^2}{m\epsilon_0}\frac{i\omega_c\omega}{(\omega^2 + i\gamma\omega - \omega_0^2)^2 - \omega_c^2\omega^2}, \tag{64}$$
$$\chi_{zz} = -\frac{Ne^2}{m\epsilon_0}\frac{1}{\omega^2 + i\gamma\omega - \omega_0^2}. \tag{65}$$

Here $\omega_c = \frac{eB}{m}$ denotes the cyclotron frequency. The off-diagonal elements χ_{xy} are typical for a magnetic medium and disappears without the magnetic field. If B is small and only terms of first order in B are included, then $\chi_{xx} = \chi_{zz}$ and $\chi_{xy} \sim B$.

Using Equation (61) together with the definition of the D-field, the linear response becomes

$$\mathbf{D} = \epsilon_0 \mathbf{E} + \mathbf{P} = \epsilon_0(1 + \chi)\mathbf{E} = \epsilon \mathbf{E}. \tag{66}$$

In gaussian units this is

$$\mathbf{D} = \mathbf{E} + 4\pi \mathbf{P} = (1 + 4\pi\epsilon_0\chi)\mathbf{E} = \epsilon \mathbf{P}, \tag{67}$$

with the dielectric function finally given by

$$\epsilon_{ij} = \delta_{ij} + 4\pi\epsilon_0\chi_{ij}. \tag{68}$$

The refraction index is related to the dielectric function through the relation $\epsilon = n^2$. In the expressions above there is resonance at frequencies close to the natural frequency, which gives the refractive index a frequency dependence and is the reason for refraction.

2.6 Magnetism

Before discussing the microscopic origin of magneto-optic effect, an explanation of the mechanisms which is the cause of magnetism is in order. The essence of magnetism can be understood by the interplay of the following three interactions[11]

- The *exchange interaction*, which stands as the strongest magnetic interaction, serves as the fundamental force behind the alignment of the spin system.
- The *spin-orbit interaction* generates orbital magnetism, couples the spin system to the lattice, and causes magnetocrystalline anisotropy.
- The *Zeeman interaction* facilitates the macroscopic alignment of spin and orbital magnetic moments, enabling measurements of the magnetic state and the creation of practical magnetic devices.

These effects will now be discussed.

2.6.1 Exchange interaction

The exchange interaction is responsible for the parallel or anti-parallel alignment of spin, i.e ferromagnetic or antiferromagnetic materials, and was first observed in the atomic spectrum of He.

This can be understood by the phenomena of identical particles, which means that one cannot distinguish between a particle a and particle b, there is no way

to put a label on them. A wave function describing two particles $\Psi(a,b)$ should then be equivalent to $\Psi(b,a)$, which leads to a wave function on the form

$$\Psi(a,b) = \frac{1}{\sqrt{2}}(\psi_1(a)\psi_2(b) \pm \psi_2(a)\psi_1(b)), \tag{69}$$

with

$$\Psi(b,a) = \pm\Psi(a,b), \tag{70}$$

which are either symmetric (+) or anti-symmetric (-) under the exchange of particles. This is formulated in the *Symmetrization Postulate* [11]

- "*If the system is totally symmetrical under the exchange of any particle pair, the particles are called bosons and obey Bose–Einstein statistics. Bosons have integer spins*"
- "*If the system is totally antisymmetrical under the exchange of any particle pair, the particles are called fermions and obey Fermi–Dirac statistics. Fermions have half-integer spins.*"

All particle systems are distinguished by this fundamental symmetry, with possible exceptions in materials of reduced dimensionality. Here exotic particles know as anyons that acquire an arbitrary phase when exchanged, has been experimentally observed[14]. Electrons are fermions and thus have an odd total wave function, which means that two electrons cannot then have identical wave functions since putting $a = b$ in Equation (69) gives $\Psi(a,a) = 0$.

The total wave function is a product of a spacial and a spin part, one of them odd, and can be written as

$$\Psi_{as}(\mathbf{a},\mathbf{b}) = \Psi_{as}(\mathbf{r}_1,\mathbf{r}_2)\chi_{sym}(\mathbf{s}_1,\mathbf{s}_2) \quad \text{or:} \quad \Psi_{sym}(\mathbf{r}_1,\mathbf{r}_2)\chi_{as}(\mathbf{s}_1,\mathbf{s}_2), \tag{71}$$

with $\Psi_{sym/as}$ having the form in Equation (69). The symmetric spin part has the form

$$\chi_{sym} = \begin{cases} \alpha\alpha \\ \frac{1}{\sqrt{2}}(\alpha\beta + \beta\alpha) \\ \beta\beta \end{cases}, \tag{72}$$

which is called the triplet state, with α and β being the eigenstate for spin up and down. The anti-symmetric spin state, called the singlet state, is

$$\chi_{as} = \frac{1}{\sqrt{2}}(\alpha\beta - \beta\alpha), \tag{73}$$

where the two spins are anti-parallel.

A strait forward calculation of the expectation value of the distance squared between two particles $\langle(\mathbf{r}_1 - \mathbf{r}_2)^2\rangle$ show that particles with an even(odd) spacial wave function lies closer(further) apart[15], which is a geometrical consequence

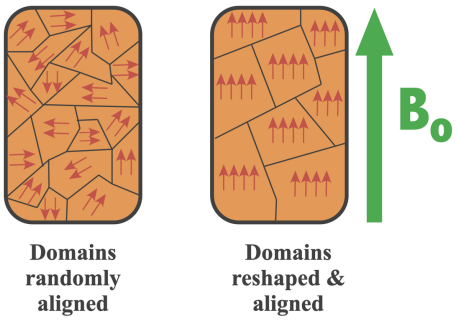

Figure 3: A schematic picture of the magnetic domains in a ferromagnet, which can be aligned by an external magnetic field due to the Zeeman effect. Courtesy of Allen D. Elster, MRIquestions.com

of the symmetrization requirement. This is what is called the exchange interaction.

Electrons with a odd spacial wave function (hence the symmetric triplet spin state χ_{sym}) feel the repulsion and thus have a larger average distance between each other than electron with an even wave function, which results in a lower potential energy from the Coulomb repulsion. To minimize energy, the spins then have a tendency to align and the effect is often described by a potential energy term

$$U = -2J\mathbf{S}_i \cdot \mathbf{S}_j, \tag{74}$$

in the Hamiltonian called the Heisenberg model. The discussion above have only been for a two particle system but the principles are generally valid and can be introduced by a Slater determinant.

The reason why not all the spins in the material are aligned is a natural consequence of the various contributions to the energy. In ferromagnetic materials which have been studied in this thesis, the material creates domains to reduce the energy of the magnetic field which is illustrated in Figure 3. By applying an external magnetic field and because of the Zeeman effect, the domains can either twist to lie in a more favourable position or the spins themselves inside the domain wall can rotate to minimize the energy. Both of which gives rise to a net magnetization in the material that can be detected through magneto-optical effects[16].

2.6.2 Spin-Orbit interaction

The spin-orbit interaction couples the spin $\mathbf{s}$ to the angular momentum $\mathbf{l}$ of the system, and this effect although being 10-100 times smaller than the exchange interaction [11], is of fundamental importance for magnetism and magneto-optical effect. It is this interaction that allows the spins and charges to communicate with each other. It couples the spin to the lattice which allows the material to

maintain a macroscopic magnetization and also, since the exchange interaction is isotropic, the SO-interaction is the main source of magnetic anisotropy.

In the Pauli equation, which one gets from the Dirac equation in the non-relativistic limit

$$(H_e + H_s)\psi = E\psi, \tag{75}$$

the first term is regular Schrödinger equation for the electron and the second term

$$H_s = \frac{e\hbar}{m_e}\mathbf{S} \cdot \mathbf{B}^*, \tag{76}$$

describes the spin energy. The magnetic field $\mathbf{B}^*$ that the electron sees as it moves is

$$\mathbf{B}^* = -\frac{\mathbf{v} \times \mathbf{E}}{2c^2}, \tag{77}$$

which is a relativistic effect and in terms of momentum and the potential field

$$\mathbf{B}^* = -\frac{\mathbf{p} \times \boldsymbol{\nabla}\phi}{2m_e c^2}. \tag{78}$$

By inserting this in Equation (76), one gets the spin-orbit Hamiltonian

$$H_{SO} = \frac{e\hbar}{2m_e^2 c^2}\mathbf{S} \cdot (\mathbf{p} \times \boldsymbol{\nabla}\phi) = -\frac{e\hbar^2}{2m_e^2 c^2}\frac{1}{r}\frac{\mathrm{d}\phi(r)}{\mathrm{d}r}\mathbf{S} \cdot \mathbf{L} = \xi_{nl}(r)\mathbf{S} \cdot \mathbf{L}. \tag{79}$$

ξ_{nl} is positive because $\frac{\mathrm{d}\phi}{\mathrm{d}r}$ is negative and is called the coupling constant[11].

This term in the Hamiltonian leads to a energy splitting, spins that are parallel or anti-parallel to the angular momentum now has different energies. As will be described below, the SO-interaction gives rise to the magneto-optic effects because the excitation from RCP and LCP light has opposite angular momenta and thus different energies.

In Section 2.5 and 2.5.1, it was shown how an external magnetic field rotates the polarization of light, but in ferromagnetic materials the effect from SO-interaction is much larger and the external field to align the spins can be ignored in calculations. It has been demonstrated experimentally that the rotation is about 1000 times larger in a ferromagnetic sample than a non-ferromagnetic one and that these effects disappears for temperatures above the Curie temperature, where the ferromagnetic properties disappears [17] [18] [19].

2.6.3 Zeeman interaction

The last interaction that will be discussed are called the Zeeman interaction. This was first observed by Pieter Zeeman in 1896, when he observed a splitting of the Na D-lines in the emission spectrum when an external magnetic field was present. The reason for this is that the electron has a magnetic moment,

which interacts with the magnetic field. This interaction can be described by the interaction Hamiltonian[11]

$$H_{Zee} = -\mathbf{m} \cdot \mathbf{H}, \tag{80}$$

where $\mathbf{H}$ is the magnetic field and $\mathbf{m}$ is the total magnetic moment which is the sum of the spin and orbital parts. Substituting for $\mathbf{m}$, one gets

$$H_{Zee} = \frac{\mu_B}{\hbar}\mathbf{H} \cdot (\mathbf{L} + 2\mathbf{S}), \tag{81}$$

or in terms if the total angular momentum $\mathbf{J} = \mathbf{L} + \mathbf{S}$,

$$\frac{\mu_B}{\hbar}\mathbf{H} \cdot (\mathbf{J} + \mathbf{S}). \tag{82}$$

This form is practical if one wants to treat the term as a perturbation of the spin-orbit Hamiltonian where the orbital angular momentum is coupled to the spin [20]. The interaction gives the angular momentum a preferred direction and causes the alignment of spin in a material to the external magnetic field (see Figure 3), which is a prerequisite to observe magneto-optic (MO) effects. It turns out that the interaction is much weaker than the spin-orbit and exchange interaction and can be treated as a perturbation when calculating the MO effects[17][19].

2.7 Microscopic perspective

The model demonstrated in Section 2.5.1 can give a good first intuition on why the MOKE and Faraday rotation take place. But one should not take this classical analogue to seriously and the whole story is of course best understood through quantum mechanics. In the above section, the three most important interactions regarding magnetism was discussed and here together with the following section, they will be related to the observed magneto-optic (MO) effects.

A first fundamental difference from the classical viewpoint is the quantized energy states and that MO effects are driven by transitions probabilities between these states. These are calculated from matrix elements of the transition matrix for the interaction and in Figure 4 (A), a perturbed charge distribution resulting in an induced electric dipole moment is illustrated. These kinds of transitions determine how easily the material is polarized and in turn results in a contribution to the diagonal elements of the dielectric function. Figure 4 (B) shows how transitions induced by RCP or LCP lead to rotation of the charge distribution, which results in off-diagonal elements and thus the MO effects if there is a difference in energy between RCP and LCP induced transitions. Under such transitions a RCP and LCP photon carries a spin of $\pm\hbar$, which get transferred to the electron in accordance to the conservation of angular momentum.

These energy splittings are illustrated in Figure 5 and occur because of the exchange and spin-orbit interaction. Figure 5(A) shows the degenerate energy levels without magnetization and Figure 5(B) illustrates how these are split into

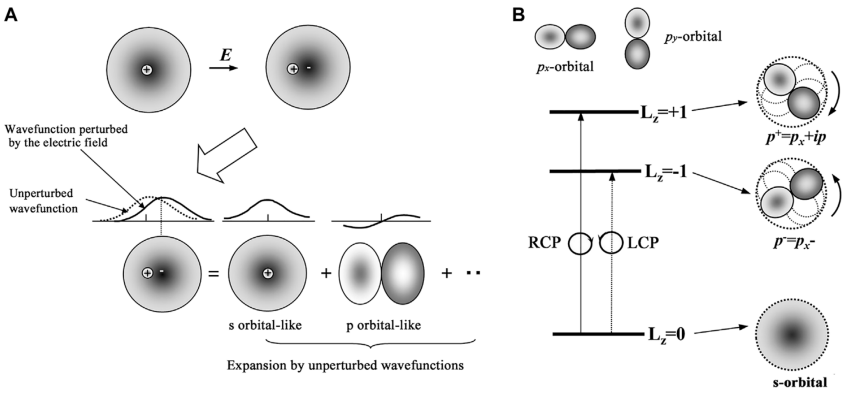

Figure 4: (A) Illustration of the altered charge distribution of an atom from a perturbation by an external electric field, inducing an electric dipole moment. This gives a contribution to the diagonal elemtents in the dielectric fucntion. (B) A schematic picture of the induced rotation by cirbular polarized light, which can be described by a superposition of p-orbitals of the form $p_\pm = p_x \pm ip_y$. By breaking of time-reversal symmetry, e.g from SO-interaction, the energy levels are shifted resulting in magneto-optical effects. "Fundamentals of Magneto-Optical Scectroscopy", K. Sato and T. Ishibashi CC BY [13]

two levels by the exchange interaction, one for spin up and one for spin down. Which level that has the lowest energy depend on the history of the material, but the splitting will happen. Finally, as the spin-orbit interaction is considered and $\mathbf{J} = \mathbf{L} + \mathbf{S}$ becomes a good quantum number, the energy levels will split further as in Figure 5(C). Left and right circular polarized light will correspond to different transitions since they carry an angular momentum of $\pm\hbar$, which gets transferred to the electron, as illustrated in the Figure. If these transitions differ in energy, the MO effects appear[13].

2.8 Optical response

2.8.1 Relating transition probability to macroscopic quantities

In the previous sections the different mechanisms that drives MO effects has been presented and also a semi-classical model was used to derive an expression for the dielectric function. Here an outline is presented on how to relate transitions probabilities calculated from quantum mechanics to the macroscopic observable effects. A possibility demonstrated by H. S. Bennett and E. A. Stern [19] is to calculate the conductivity tensor and then relate it to the current density. With

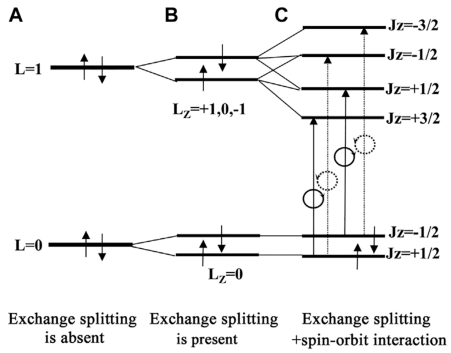

Figure 5: Schematic picture of the energy shifts due to exchange splitting and SO-interaction, resulting in MO effects. "Fundamentals of Magneto-Optical Scectroscopy", K. Sato and T. Ishibashi CC BY [13]

cubic symmetry, the conductivity tensor has the form

$$\sigma = \begin{pmatrix} \sigma_{xx} & \sigma_{xy} & 0 \\ -\sigma_{xy} & \sigma_{xx} & 0 \\ 0 & 0 & \sigma_{zz} \end{pmatrix}. \tag{83}$$

For a homogeneous, time-dependent medium, the current can be written in the form

$$J_i = \sum_j \sigma_{ij} E_j. \tag{84}$$

If the electric field is RCP/LCP, mathematically written as $\mathbf{E}_{r/l} = (\hat{\mathbf{x}} \pm i\hat{\mathbf{y}})Ee^{-i\omega t}$, then the current is given by

$$\mathbf{J}_{r/l} = \sigma \mathbf{E}_{r/l} = (\sigma_{xx} \pm i\sigma_{xy})\mathbf{E}_{r/l} = \sigma_{r/l}\mathbf{E}_{r/l}, \tag{85}$$

where r/l stands for right/left circularly polarized. The current, and hence the conductivity tensor, can be related to the absorbed energy through the equation for power

$$P = \frac{1}{2}\int \mathrm{Re}\{\mathbf{J}^* \cdot \mathbf{E}\} dV, \tag{86}$$

and if one neglects space variation of $\mathbf{E}$, which is reasonable for wavelength large compared to the inter-atomic distance, we can rewrite this as

$$P = \frac{1}{2} V \,\mathrm{Re}\left\{ \sum_{i,j} \sigma_{ij}^* E_j^* E_i \right\}, \tag{87}$$

with

$$\sigma_{ij} = \sigma_{1ij} + i\sigma_{2ij}, \tag{88}$$

denoting the real and imaginary part of each matrix element. For linear polarized electric field, the power becomes

$$P_x = \frac{1}{2} V E^2 \sigma_{1xx} \tag{89}$$

and for right (r) or left (l) circular polarized light

$$P_{r/l} = \frac{1}{2} E^2 (\sigma_{1xx} \mp \sigma_{2xy}). \tag{90}$$

These equations can then be combined to get an expression for the real part of σ_{xx} and imaginary part of σ_{xy} as follows

$$\sigma_{1xx} = \frac{2}{VE^2} P_x = \frac{1}{VE^2}(P_r + P_l), \tag{91}$$

$$\sigma_{2xy} = \frac{1}{VE^2}(P_l - P_r). \tag{92}$$

Now there is a useful relation from complex analysis called the Kramers-Kronig relations which relates the real and imaginary part of a complex function, given that the function is analytic in the closed upper half plane and that the function vanishes faster than $1/|z|$ as $z \to \infty$. If $f(z) = f_1(z) + if_2(z)$ is the real and imaginary part of the complex valued function f and z is a complex variable, the relations are

$$f_1(z) = \frac{1}{\pi} \mathcal{P} \int_{-\infty}^{\infty} \frac{f_2(z')}{z' - z}\, dz', \tag{93}$$

$$f_2(z) = -\frac{1}{\pi} \mathcal{P} \int_{-\infty}^{\infty} \frac{f_1(z')}{z' - z}\, dz'. \tag{94}$$

By conservation of energy and causality, H. S. Bennett and E. A. Stern [19] argue that σ_{ij} satisfies the conditions necessary to use these relations in order to calculate the other part of the conductivity tensor. What is left is to calculate $P_{x/r/l}$ which can be done with the relation

$$P d\omega = \hbar\omega \sum_i W_i, \tag{95}$$

where W_i is the probability per unit time that a process that absorbs energy in the interval $(\hbar\omega, \hbar\omega + \hbar d\omega)$ happen. This transition probability can then be calculated with quantum mechanics in order to determine the conductivity tensor.

2.8.2 Transition probability with time-dependent perturbation theory

The transition probabilities W_i in Equation (95) can be calculated with time-dependent perturbation theory. In order to do this, the eigenstates to the unperturbed Hamiltonian needs to be found and then the matrix elements for the transitions can be calculated with Fermi's golden rule.

First, the Hamiltonian for an electron in a solid with a optical field present can be written as [7]

$$H = \frac{(\mathbf{p} - e\mathbf{A})^2}{2m} + V(\mathbf{r}) = \frac{p^2}{2m} - \frac{e\mathbf{p}\cdot\mathbf{A}}{m} + \frac{e^2A^2}{2m} + V(\mathbf{r}), \tag{96}$$

$$= H_0 - \frac{e\mathbf{p}\cdot\mathbf{A}}{m} + \frac{e^2A^2}{2m} \tag{97}$$

with $V(\mathbf{r})$ being the potential from the material and $V(\mathbf{r})$ the magnetic vector potential from the radiation. Here the Coulomb gauge was chosen ($\boldsymbol{\nabla}\cdot\mathbf{A} = 0$) in order for $\mathbf{p}$ and $\mathbf{A}$ to commute. $H_0 = \frac{p^2}{2m} + V(\mathbf{r})$ is the unperturbed Hamiltonian and the other terms is treated as a perturbation H' from the optical field. Although this Hamiltonian can be used to calculate transition probabilities, in order to capture the magneto-optical effects, spin and it's interaction with the electric field needs to be considered.

What additionally needs to be considered is the applied uniform magnetic field that align the spins and the SO-interaction. This can be done by the substitution $\mathbf{p} \to \boldsymbol{\pi}$, where $\boldsymbol{\pi}$ is

$$\boldsymbol{\pi} = \mathbf{P} + \frac{\hbar}{4mc^2}\boldsymbol{\sigma} \times \boldsymbol{\nabla}V, \tag{98}$$

$$\mathbf{P} = \mathbf{p} + \frac{e}{c}\mathbf{A}_M, \tag{99}$$

here $\mathbf{A}_M$ is the vector potential for the uniform magnetic field and V is the potential and $\boldsymbol{\sigma}$ is the Pauli spin operator. The full Hamiltonian, when summing over all electrons, can then be written as

$$H = H_0 + \sum_i \frac{e}{mc}\boldsymbol{\pi}_i \cdot \mathbf{A}_L(\mathbf{r}_i) + \frac{e^2}{2m^2c^2}A_L^2(\mathbf{r}_i), \tag{100}$$

which is similar to Equation (97). Here $\mathbf{A}_L$ is the vector potential from the optical field. By assuming that each electron interacts with an effective mean field, $H_0 = \sum_i H_{0i}$ with

$$H_{0i} = \frac{P_i^2}{2m} + V(\mathbf{r}_i) + \frac{\hbar}{4m^2c^2}\mathbf{P}_i \cdot [\boldsymbol{\sigma} \times \boldsymbol{\nabla}V(\mathbf{r}_i)] + V_{eff}(\mathbf{r}_i). \tag{101}$$

The third term comes from the SO-interaction which is a relativistic effect and describes the interaction between the spin of the electron and the effective magnetic field it sees when it moves in the potential. If the spherically symmetric

term of the potential is dominant, this interaction term can be modified to the form familiar in the hydrogen atom

$$H_{SO} = \xi_l \mathbf{L} \cdot \mathbf{S}, \tag{102}$$

where ξ_l is the strength of the interaction. Now the total Hamiltonian can be written as

$$H = \sum_i H_i = \sum_i H_{0i} + H_i', \tag{103}$$

where the last term is the perturbation in Equation (100). By only considering the terms linear in $\mathbf{A}_L$, since the perturbation is assumed to be weak, one gets

$$H_i' = \frac{e}{mc} \boldsymbol{\pi}_i \cdot \mathbf{A}_L(\mathbf{r}_i). \tag{104}$$

Using first order time-dependent perturbation theory, the transition probability per unit time from an initial state $|i\rangle$ to a final state $|f\rangle$ (for a plane wave in x-direction), is given by Fermi's golden rule

$$W_{fi} = \frac{2\pi}{\hbar} \frac{E^2 e^2}{4m^2\omega^2} |\langle f| \pi_x |i\rangle|^2 (\delta(\varepsilon_f - \varepsilon_i \pm \hbar\omega). \tag{105}$$

Here π_x is the x-component of the kinetic momentum operator and $\varepsilon_{i/f}$ is the energy of the initial and final state. The δ is the dirac delta function. By combining this equation with the relations in Equation (91) and (95) and summing over all initial and final states, the real part of σ_{xx} can be written as

$$\sigma_{1xx} = \frac{\pi e^2}{\omega m^2 V} \sum_{i,occ} \sum_{f,unocc} |\langle f| \pi_x |i\rangle|^2 \delta(\varepsilon_f - \varepsilon_i \pm \hbar\omega). \tag{106}$$

The summation here is over all occupied initial states and all unoccupied final states. The real part can then be calculated with the Kramers-Kronig relation. The expression for RCP and LCP light is similar, with π_x replaced by $\pi^{\pm} = \pi_x \pm i\pi_y$ and some of the coefficients changed. This was just an overview to get an intuition for how one goes about calculating the conductivity tensor. For a detailed derivation see reference [19] and for a more modern approach see reference [21], where Kubo's formula is used together with another integration technique that does not have to resort to the Kramers-Kronig relations. What is important is that because of the symmetry breaking due to the net spin in the material, the induced current from RCP and LCP light is different. This then result in the off-diagonal elements σ_{xy} which in turn rotates the polarization of the incident light.

When Fermi's golden rule was used above, it was assumed that the unperturbed eigenstates where known. To find these is a non-trivial problem since the Hamiltonian is a complicated many-body problem. In order to solve this, people resort to elaborate methods such as density funcitonal theory.

2.9 Density functional theory (DFT)

The Lorentz model used above is of course a very crude approximation. In reality, the situation is much more complicated. Firstly, the electrons in the atom forms complicated orbitals and they can get excited to a higher unoccupied energy state given the right amount of energy. The outer most electrons also form bonds with neighbouring atoms and the electrons carry spin. There are also many types of interactions to consider such as spin-orbit interaction and interaction with collective excitations such as phonons and magnons.

A more realistic way of finding the optical response of the system would be to first solve the Schrödinger equation for the system and then perturb it using perturbation theory. But even when only considering the Coulomb interaction, the problem is still very hard. The time independent Schrödinger equation (in atomic units) that needs to be solved is

$$\left(-\sum_i \frac{1}{2}\nabla_i^2 - \sum_I \frac{1}{2M_I}\nabla_I^2 + \frac{1}{2}\sum_{i\neq j} \frac{1}{|\mathbf{r}_i - \mathbf{r}_j|} \right. \tag{107}$$

$$\left. + \sum_{I\neq J} \frac{Z_I Z_J}{|\mathbf{R}_I - \mathbf{R}_J|} - \sum_{i,I} \frac{Z_I}{|\mathbf{r}_i - \mathbf{R}_I|} \right) \Psi(\mathbf{r}, \mathbf{R}) = E_{tot}\Psi(\mathbf{r}, \mathbf{R}). \tag{108}$$

Here the small and big indices represent sum over electrons respectively nuclei. The first two terms are the kinetic energies for the electrons and nuclei. The third and forth term is the Coulomb repulsion for for electron-electron and nucei-nuclei with the factor $\frac{1}{2}$ because it sums over each pair twice. The last term is attractive Coulomb force between the electrons and nuclei and Z_I is the charge of nuclei I. The number of degrees of freedom grows exponentially as the number of atoms in the system increases and the problem becomes impossible to solve analytically, even numerically, in a realistic material. A first approximation that is usually done is the Born-Oppenheimer approximation[22].

This approximation is based on the large difference in mass between the electron and the nucleus. The electrons thus moves much faster and in their frame of reference, the nuclei looks to be fixed in place. This is called the clamped nuclei approximation. To the nucleus, the electrons behaves as responding instantaneously to any movement. Because of the difference in time-scales the Schrödinger equation can be separately solved for the electrons, with the kinetic energy of the nuclei set to zero and their positions $\mathbf{R}_I$ held fixed. The

Scrödinger equation for the electrons then becomes [23]

$$\left(-\sum_i \frac{1}{2}\nabla_i^2 - \sum_{i,I} \frac{Z_I}{|\mathbf{r}_i - \mathbf{R}_I|} + \frac{1}{2}\sum_{i \neq j} \frac{1}{|\mathbf{r}_i - \mathbf{r}_j|} \right) \Psi_{elec}(\mathbf{r}) = E_{elec}\Psi_{elec}(\mathbf{r}), \tag{109}$$

$$E_{elec} = \left(E_{tot} - \sum_{I \neq J} \frac{Z_I Z_J}{|\mathbf{R}_I - \mathbf{R}_J|} \right). \tag{110}$$

Here the Coulomb repulsion for the nuclei is constant and is included in the energy. The solution to this equation then give constant energy surfaces that depends on the coordinates of the nuclei and can be used as a potential when solving that part.

Even with the Born-Oppenheimer approximation the problem is hard because of the third term in the Hamiltonian that is the interaction between all the electrons. This is called a many-body problem and a general closed-form solution doesn't even exist for three bodies. Despite this, people run quantum mechanical calculations and simulations for large structures and the key is density functional theory. The details is outside the scope of this thesis, but the qualitative approach will be explained here, since dielectric functions from such calculations are used in the calculations for the result.

A first step is to notice that the actual wave function of the electrons cannot be measured, what can be measured however is the number of electrons at a certain position which is related to the density. By assuming that the electrons are non-interacting, or interact with a mean-field, the wave function can be simplified as

$$\Psi(\mathbf{r}_1, \mathbf{r}_2, ..., \mathbf{r}_N) = \psi_1(\mathbf{r}_1)\psi_2(\mathbf{r}_2)...\psi_N(\mathbf{r}_N). \tag{111}$$

The electronic density can then be written as

$$n(\mathbf{r}) = 2\sum_i |\psi_i(\mathbf{r})|^2, \tag{112}$$

which only depends on three instead on 3N coordinates. The power of DFT comes from the possibility of relating measurable observables to the density. This is possible because of the following two important theorems known as the Hohenberg-Kohn theorems [23]:

1. The ground-state energy E in the Schrödinger equation is a unique functional of the electron density $n(\mathbf{r})$.

2. The electron density that minimizes the energy of the overall functional is the true electron density corresponding to the full solution of the Schrödinger equation.

The first theorem tells us that there exists a one-to-one mapping between the ground state wave function and the ground state density and the energy can be written as $E = E(n(\mathbf{r}))$. This is a functional, which is similar to a function, but instead takes a function as an input and returns a number. In this case given a electronic density it returns an energy. This is why it is called density functional theory. What the theorem doesn't say is the form of the functional. The second theorem states the useful property of the functional that if the functional was known, then the electronic density could be found by varying it until a minima is reached. This fact is used with numerical methods which iterate until a satisfactory precision is reached.

But to find the density in Equation (112) the single-electron wave functions are needed. A way to do this is through the Kohm-Sham equations

$$\left(-\frac{1}{2}\nabla^2 + V_n(\mathbf{r}) + V_H(\mathbf{r}) + V_{XC}(\mathbf{r})\right)\psi_i(\mathbf{r}) = \varepsilon_i\psi_i(\mathbf{r}), \tag{113}$$

which is similar to the Equation (109) but without the sum over all interaction between the electrons. The term V_n is the interaction of a single electron with the nuclei, similarly to Equation (109). The term V_H is called the Hartree potential

$$V_H(\mathbf{r}) = \int \frac{n(\mathbf{r}')}{|\mathbf{r} - \mathbf{r}'|} d\mathbf{r}', \tag{114}$$

which describes the interaction between the single electron and the electronic density. The last term V_{XC} is called the exchange-correlation term and contains all other effects and is written as the functional derivative of the exchange correlation energy

$$V_{XC}(\mathbf{r}) = \frac{\delta E_{XC}[n(\mathbf{r})]}{\delta n(\mathbf{r})}. \tag{115}$$

If E_{XC} is known, then the problem could be solved exactly. This has never been done, but there are many approximations of the exchange-correlation which can be used.

To solve a problem the procedure is the following. First, do an initial guess of the density $n(\mathbf{r})$. Then, solve the Kohm-Sham equations with this trial density. The solutions ψ_i can then be used to calculate a new density with Equation (112). This density is then compared with the old one and if they are the same, this is ground state density. Otherwise, the density is adjusted somehow and the whole procedure is started over.

3 Transfer matrix methods

Optical problems with multiple double refracting layers are complicated to solve because of the internal reflections illustrated in Figure 6. A practical method to solve such a problem is by transfer matrices, where a total transfer matrix T is

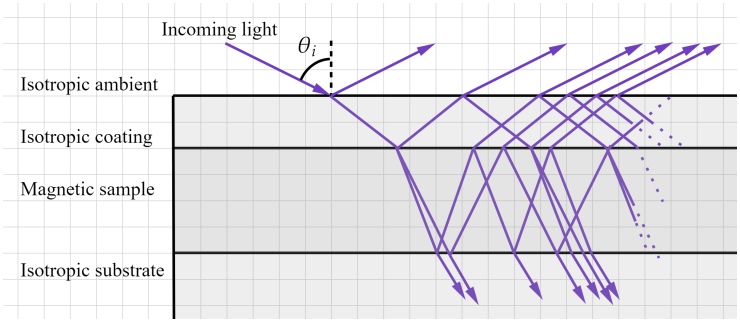

Figure 6: Illustration of the multiple reflections involved when studying layered media. Note that the light ray split into two eigenmodes when entering the magnetic sample

calculated from the product of the partial transfer matrices for each layer. It is convenient not only because the transfer matrix can be calculated for each layer separately and then combined in various ways, but also because the calculations becomes tidier and it is easier to get an overview on what is going on. Further more, the incoming light do not have to be considered and the calculations can be done solely with the elements in the setup.

The method was first introduced by Jones [24] and Abelès [25] with a 2x2 matrix calculus which will be illustrated below. This approach uses the fact that the electric and magnetic field decouples to the wave equations (Equation (20-21)) hence only two field components needs to be carried through the calculations, e.g (E_x, E_y) or (E_x, H_x), as two component vectors. The **E** or **H** field can then be derived from Maxwell's equations if needed.

For simplicity, let us assume normal incidence in the z-direction and that the index of refraction is different for the field oscillating in the x- respectively y-direction, denoted by N_x and N_y. The electric field in the x-direction can then be written as

$$E_x(z) = E_{x0} e^{i(k_0 N_x z - \omega t)}, \qquad k_0 = \frac{\omega}{c}, \tag{116}$$

$$E_x(z+d) = E_{x0} e^{i(k_0 N_x (z+d) - \omega t)} = E_x(z) e^{i k_0 N_x d}. \tag{117}$$

This can similarly be done for the y-component. With matrices, this can be written as

$$\begin{pmatrix} E_x(z+d) \\ E_y(z+d) \end{pmatrix} = \begin{pmatrix} e^{i k_0 N_x d} & 0 \\ 0 & e^{i k_0 N_y d} \end{pmatrix} \begin{pmatrix} E_x(z) \\ E_y(z) \end{pmatrix} \tag{118}$$

This matrix is a transfer matrix which "transfer" the electric field a distance d along the z-axis. Here, the materials principle axes are in the x and y-direction. More generally, these are at an angle θ from the "laboratory" coordinate system.

It is then possible to write the transform matrix as

$$T(d) = R \begin{pmatrix} e^{ik_0 N_x d} & 0 \\ 0 & e^{ik_0 N_y d} \end{pmatrix} R^{-1}, \tag{119}$$

with

$$R = \begin{pmatrix} \cos\theta & -\sin\theta \\ \sin\theta & \cos\theta \end{pmatrix} \tag{120}$$

If there is no surface charge nor surface current in the media, the electric field is continuous across a boundary (see Equations (7-8)). Then we have the equation

$$\boldsymbol{\varepsilon}_1 = T(d)\boldsymbol{\varepsilon}_0, \tag{121}$$

where $\boldsymbol{\varepsilon}_i$ are the electric field components before and after an optical system.

If the total system contains a composition of different optical systems, one can multiply the individual transfer matrices to get a total transfer matrix

$$\boldsymbol{\varepsilon}_f = T\boldsymbol{\varepsilon}_i, \quad T = \prod_{i=1}^{N} T_i(d_i). \tag{122}$$

Once this matrix is found, the problem is solved and the method above can be extended to problems concerning reflection as well. But for a more general theoretical framework, one needs to introduce 4×4 - matrices.

3.1 The general transfer matrix

The matrix method introduced by Jones and Abelès illustrates the convenience in using a transfer matrix method to solve optical problems. But for situations where the symmetry of the medium is low, or when magnetic mediums are considered, the method becomes impractical and a generalization to 4×4 - matrices is convenient. In this sections a general approach will be presented where a total transfer matrix

$$T = A_i^{-1}(\prod_{j=1}^{n} T_{pj})\, A_f \tag{123}$$

is calculated from a product of the partial transfer matrices T_{pj} for each layer. In the literature, there are several variations but the overall strategy is the same, see for example [26],[27],[28] and [29].

The A matrices are called boundary matrices and projects the p- and s-components of the light wave onto the x- and y-components to fulfill the boundary condition that says that the field components parallel to a surface is continuous across that boundary (Equations (7-8)). Equation (123) is illustrated graphically in Figure 7.

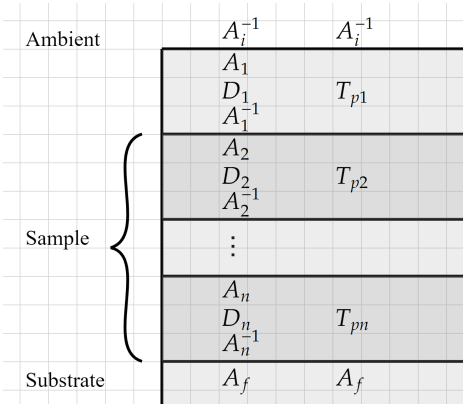

Figure 7: Graphic representation of the matrix method (see Equation (123) and (217)).

The total transfer matrix T relates the fields before and after the layered medium with the relation

$$P_i = TP_f, \tag{124}$$

where the subscript i and f stands for initial and final field vector. Explicitly, these are

$$\begin{pmatrix} E_{is} \\ E_{rs} \\ E_{ip} \\ E_{rp} \end{pmatrix} = T \begin{pmatrix} E_{ts} \\ 0 \\ E_{tp} \\ 0 \end{pmatrix} = \begin{pmatrix} T_{11} & T_{12} & T_{13} & T_{14} \\ T_{21} & T_{22} & T_{23} & T_{24} \\ T_{31} & T_{32} & T_{33} & T_{34} \\ T_{41} & T_{42} & T_{43} & T_{44} \end{pmatrix} \begin{pmatrix} E_{ts} \\ 0 \\ E_{tp} \\ 0 \end{pmatrix}. \tag{125}$$

From this equation all measurable optical constants can be deduced. For an isotropic medium, there is four Fresnel equations, reflection and transmission for p- and s-polarized waves. In the case of anisotropic media the polarization

mix, resulting in the eighth combinations[29][30]

$$r_{pp} = \left(\frac{E_{rp}}{E_{ip}}\right)_{E_{is}=0} = \frac{T_{11}T_{43} - T_{13}T_{41}}{T_{11}T_{33} - T_{13}T_{31}}, \tag{126}$$

$$r_{sp} = \left(\frac{E_{rs}}{E_{ip}}\right)_{E_{is}=0} = \frac{T_{11}T_{23} - T_{13}T_{21}}{T_{11}T_{33} - T_{13}T_{31}}, \tag{127}$$

$$r_{ss} = \left(\frac{E_{rs}}{E_{is}}\right)_{E_{ip}=0} = \frac{T_{21}T_{33} - T_{23}T_{31}}{T_{11}T_{33} - T_{13}T_{31}}, \tag{128}$$

$$r_{ps} = \left(\frac{E_{rp}}{E_{is}}\right)_{E_{ip}=0} = \frac{T_{33}T_{41} - T_{31}T_{43}}{T_{11}T_{33} - T_{13}T_{31}}, \tag{129}$$

$$t_{pp} = \left(\frac{E_{tp}}{E_{ip}}\right)_{E_{is}=0} = \frac{T_{11}}{T_{11}T_{33} - T_{13}T_{31}}, \tag{130}$$

$$t_{sp} = \left(\frac{E_{ts}}{E_{ip}}\right)_{E_{is}=0} = \frac{-T_{13}}{T_{11}T_{33} - T_{13}T_{31}}, \tag{131}$$

$$t_{ss} = \left(\frac{E_{ts}}{E_{is}}\right)_{E_{ip}=0} = \frac{T_{33}}{T_{11}T_{33} - T_{13}T_{31}}, \tag{132}$$

$$t_{ps} = \left(\frac{E_{tp}}{E_{is}}\right)_{E_{ip}=0} = \frac{-T_{31}}{T_{11}T_{33} - T_{13}T_{31}}. \tag{133}$$

One can also derive the Fresnel coefficients by writing $P_i = (E_{si}, E_{pi}, E_{sr}, E_{pr}) = (\mathbf{E}_i, \mathbf{E}_r)$ and $P_f = (E_{st}, E_{pt}, 0, 0) = (\mathbf{E}_t, 0)$ and the T matrix as a four 2×2 block matrices

$$\begin{pmatrix} \mathbf{E}_i \\ \mathbf{E}_r \end{pmatrix} = \begin{pmatrix} G & H \\ I & J \end{pmatrix} \begin{pmatrix} \mathbf{E}_t \\ 0 \end{pmatrix}. \tag{134}$$

Then

$$\mathbf{E}_t = G^{-1}\mathbf{E}_i \tag{135}$$

$$\mathbf{E}_r = I\mathbf{E}_t = IG^{-1}\mathbf{E}_i, \tag{136}$$

and finally

$$\begin{pmatrix} t_{ss} & t_{sp} \\ t_{ps} & t_{pp} \end{pmatrix} = G^{-1}, \tag{137}$$

$$\begin{pmatrix} r_{ss} & r_{sp} \\ r_{ps} & r_{pp} \end{pmatrix} = IG^{-1}. \tag{138}$$

The magneto-optic Kerr effect or Faraday rotation can be calculated from ratios of these coefficients.

3.2 The Partial Transfer Matrix

Two different approaches to calculate the partial transfer matrix in Equation (123) will be presented which I will call the differential approach and the

magneto-optic approach. Which one to use depend on three things; the form of the dielectric function, if the assumption that the permeability $\mu = 1$ is valid and that the medium is non-gyroscopic. The two latter conditions are often met, but to have

$$\varepsilon = \begin{pmatrix} \varepsilon_{xx} & \varepsilon_{xy} & \varepsilon_{xz} \\ \varepsilon_{yx} & \varepsilon_{yy} & \varepsilon_{yz} \\ \varepsilon_{zx} & \varepsilon_{zy} & \varepsilon_{zz} \end{pmatrix} \xrightarrow{?} \varepsilon = N^2 \begin{pmatrix} 1 & iQ & 0 \\ -iQ & 1 & 0 \\ 0 & 0 & 1 \end{pmatrix}, \tag{139}$$

cubic symmetry is often required [19] and the form to the right in Equation (139) is required for the magneto-optic approach. In the form written here, the magnetization is in the z-direction but it can be rotated to an arbitrary direction with the Euler angles [31]. If these three conditions are met, the magneto-optic approach can be used, otherwise one has to resort to the differential one.

In this section the general differential approach will be presented first, followed by the magneto-optic approach which was implemented in Python and used for the calculations in the result.

3.3 Differential Approach

The derivation of the differential approach will follow the one by D. W. Berreman [32], and starts from Maxwell's equations in matrix form

$$\begin{pmatrix} 0 & 0 & 0 & 0 & -\frac{\partial}{\partial z} & \frac{\partial}{\partial y} \\ 0 & 0 & 0 & \frac{\partial}{\partial z} & 0 & -\frac{\partial}{\partial x} \\ 0 & 0 & 0 & -\frac{\partial}{\partial y} & \frac{\partial}{\partial x} & 0 \\ 0 & \frac{\partial}{\partial z} & -\frac{\partial}{\partial y} & 0 & 0 & 0 \\ -\frac{\partial}{\partial z} & 0 & \frac{\partial}{\partial x} & 0 & 0 & 0 \\ \frac{\partial}{\partial y} & -\frac{\partial}{\partial x} & 0 & 0 & 0 & 0 \end{pmatrix} \begin{pmatrix} E_x \\ E_y \\ E_z \\ H_x \\ H_y \\ H_z \end{pmatrix} = \frac{1}{c}\frac{\partial}{\partial t} \begin{pmatrix} D_x \\ D_y \\ D_z \\ B_x \\ B_y \\ B_z \end{pmatrix}. \tag{140}$$

Following his notation, Equation (140) will be written as

$$\mathbf{RG} = \frac{1}{c}\frac{\partial}{\partial t}\mathbf{C}. \tag{141}$$

One can first note that $\mathbf{R}$ is symmetric, with the off-diagonal blocks being the curl operator. By assuming a linear response, it is possible to write the relation

$$\mathbf{C} = \mathbf{MG}, \tag{142}$$

where $\mathbf{M}$ is a 6×6 - matrix containing ϵ and μ, but also the off-diagonal terms which are called optical-rotation tensors that couple $\mathbf{D}$ with $\mathbf{H}$ and $\mathbf{B}$ with $\mathbf{E}$. It is explicitly written as

$$\mathbf{M} = \begin{pmatrix} \boldsymbol{\epsilon} & \boldsymbol{\rho} \\ \boldsymbol{\rho'} & \boldsymbol{\mu} \end{pmatrix} = \begin{pmatrix} \epsilon_{11} & \epsilon_{12} & \epsilon_{13} & \rho_{11} & \rho_{12} & \rho_{13} \\ \epsilon_{21} & \epsilon_{22} & \epsilon_{23} & \rho_{21} & \rho_{22} & \rho_{23} \\ \epsilon_{31} & \epsilon_{32} & \epsilon_{33} & \rho_{31} & \rho_{32} & \rho_{33} \\ \rho'_{11} & \rho'_{12} & \rho'_{13} & \mu_{11} & \mu_{12} & \mu_{13} \\ \rho'_{21} & \rho'_{22} & \rho'_{23} & \mu_{21} & \mu_{22} & \mu_{23} \\ \rho'_{31} & \rho'_{32} & \rho'_{33} & \mu_{31} & \mu_{32} & \mu_{33} \end{pmatrix}. \tag{143}$$

Equation (141) then becomes

$$\mathbf{RG} = \frac{1}{c}\frac{\partial}{\partial t}\mathbf{MG}. \tag{144}$$

This can further be simplified by assuming an optical disturbance (i.e light that hits the material) with frequency ω. The field will thus have a factor $\exp(-i\omega t)$ as time-dependence and the equation becomes

$$\mathbf{R\Gamma} = -\frac{i\omega}{c}\mathbf{M\Gamma}, \tag{145}$$

with $\mathbf{\Gamma}$ being the spacial part. By assuming that light is incident in the x-z-plane and that $\mathbf{M}$ is a function of z only, $\mathbf{\Gamma}$ will have a factor $\exp(i\xi x)$ as the only x-dependence and no y-dependence. This assumption simplifies the curl operator in the $\mathbf{R}$ matrix

$$\mathbf{R} = \begin{pmatrix} 0 & 0 & 0 & 0 & -\frac{\partial}{\partial z} & 0 \\ 0 & 0 & 0 & \frac{\partial}{\partial z} & 0 & -i\xi \\ 0 & 0 & 0 & 0 & i\xi & 0 \\ 0 & \frac{\partial}{\partial z} & 0 & 0 & 0 & 0 \\ -\frac{\partial}{\partial z} & 0 & i\xi & 0 & 0 & 0 \\ 0 & -i\xi & 0 & 0 & 0 & 0 \end{pmatrix}, \tag{146}$$

where the third and sixth row are just linear algebraic equations. So two of the six components can be solved for and thus be eliminated and they are chosen to be the E_z and H_z components. After simplification, what's left is four first order linear differential equations

$$\frac{\partial}{\partial z}\begin{pmatrix} E_x \\ E_y \\ H_x \\ H_y \end{pmatrix} = i\frac{\omega}{c}\begin{pmatrix} \Delta_{11} & \Delta_{12} & \Delta_{13} & \Delta_{14} \\ \Delta_{21} & \Delta_{22} & \Delta_{23} & \Delta_{24} \\ \Delta_{31} & \Delta_{32} & \Delta_{33} & \Delta_{34} \\ \Delta_{41} & \Delta_{42} & \Delta_{43} & \Delta_{44} \end{pmatrix}\begin{pmatrix} E_x \\ E_y \\ H_x \\ H_y \end{pmatrix}, \tag{147}$$

where Δ_{ij} are given explicitly in terms of the M_{ij}'s (see Section 9.1 in Appendix). This equation will simply be written as

$$\frac{\partial}{\partial z}\psi = ik_0\Delta\psi, \quad k_0 \equiv \frac{\omega}{c}, \tag{148}$$

and says how the electromagnetic field changes when propagating in the z-direction. The main task is to solve this equation and if Δ does not depend on z, the solution is

$$\psi(z+d) = e^{ik_0\Delta d}\psi(z) = T_p(d)\psi(z), \tag{149}$$

where $\mathbf{T}_p$ is the partial transfer matrix in Equation (123) and is defined as

$$T_p(d) = e^{ik_0\Delta d}. \tag{150}$$

The main problem then boils down to calculate this matrix for a given $\mathbf{M}$ and if the medium is not homogeneous, it's possible to approximate it as a finite number of homogeneous slabs, each with it's own partial transfer matrix.

There are three main ways to calculate this matrix. Firstly, one can simply write Equation (150) as the power series

$$e^{ik_0\Delta d} = \mathbb{1} + ik_0\Delta d + \frac{1}{2!}(ik_0\Delta d)^2 + \frac{1}{3!}(ik_0\Delta d)^3 + ..., \tag{151}$$

up to some order. For a thin slab this series may be truncated for a sufficiently small d. In some cases where the symmetry is high, it is possible to write this series in a closed form.

If this is not possible, one can find the four eigenvalues of Δ by solving the secular equation

$$\det(\Delta - q_k\mathbb{1}) = 0, \tag{152}$$

and then find the eigenvectors $\boldsymbol{\psi}_k$ by solving

$$\Delta\boldsymbol{\psi}_k = q_k\boldsymbol{\psi}_k. \tag{153}$$

Now, a matrix function is defined through its series expansion. So it's easy to verify that

$$e^{ik_0\Delta d}\boldsymbol{\psi}_k = \sum_{n=0}^{\infty}\frac{1}{n!}(ik_0\Delta d)^n\boldsymbol{\psi}_k = \sum_{n=0}^{\infty}\frac{1}{n!}(ik_0q_k d)^n\boldsymbol{\psi}_k = e^{ik_0q_k d}\boldsymbol{\psi}_k. \tag{154}$$

By constructing a matrix

$$\boldsymbol{\Psi} = \begin{pmatrix} | & | & | & | \\ \boldsymbol{\psi}_1 & \boldsymbol{\psi}_2 & \boldsymbol{\psi}_3 & \boldsymbol{\psi}_4 \\ | & | & | & | \end{pmatrix}, \tag{155}$$

with the eigenvectors as columns vectors and acting with the transfer matrix

$$\mathbf{T}_p(d)\boldsymbol{\Psi} = e^{ik_0\Delta d}\boldsymbol{\Psi} = \begin{pmatrix} | & | & | & | \\ e^{ik_0\Delta d}\boldsymbol{\psi}_1 & e^{ik_0\Delta d}\boldsymbol{\psi}_2 & e^{ik_0\Delta d}\boldsymbol{\psi}_3 & e^{ik_0\Delta d}\boldsymbol{\psi}_4 \\ | & | & | & | \end{pmatrix} \tag{156}$$

$$= \begin{pmatrix} | & | & | & | \\ e^{ik_0q_1 d}\boldsymbol{\psi}_1 & e^{ik_0q_2 d}\boldsymbol{\psi}_2 & e^{ik_0q_3 d}\boldsymbol{\psi}_3 & e^{ik_0q_4 d}\boldsymbol{\psi}_4 \\ | & | & | & | \end{pmatrix} = \boldsymbol{\Psi}\mathbf{K}(d). \tag{157}$$

So the transfer matrix can be written as

$$\mathbf{T}_p(d) = \boldsymbol{\Psi}\mathbf{K}(d)\boldsymbol{\Psi}^{-1}, \tag{158}$$

where $\mathbf{K}(d)$ is a diagonal matrix with $\exp(ik_0q_k d)$ as elements.

The third possibility was introduced by Wöhler *et. al* and make is of Cayley-Hamiltons theorem[33]. The theorem states that a matrix function can be represented as a finite series of order n, where n is the size of the square matrix. They showed that the partial transfer matrix can be written as

$$e^{ik_0\Delta d} = \beta_0\mathbb{1} + \beta_1\Delta + \beta_2\Delta^2 + \beta_3\Delta^3, \tag{159}$$

where the constants β_i are defined by the four equations

$$e^{ik_0 q_k d} = \beta_0 + \beta_1 q_k + \beta_2 q_k^2 + \beta_3 q_k^3, \quad k = 1, ..., 4, \tag{160}$$

with q_k being the eigenvalues of Δ. This exact expression for $\mathbf{T}_p$ allows one to do a single calculation for thick slabs, in contrast to the series expansion which can only be calculated for small d's which requires many calculations over the whole slab.

M. Schubert [26] explicitly calculated the eigenvalues in the case for non-magnetic ($\boldsymbol{\mu} = \mathbb{1}$) and non-gyrotropic ($\boldsymbol{\rho} = \mathbf{0}$) media, with a symmetric dielectric function ($\epsilon_{ij} = \epsilon_{ji}$). This together with Equation (159), gives an exact form of the partial transfer matrix.

3.3.1 Simplifying assumptions for Δ

With the assumption that the media is nonmagnetic, $\boldsymbol{\mu} = \mathbb{1}$ and nongyrotropic, $\boldsymbol{\rho} = \mathbb{0}$, Δ in Equation (148) becomes [26]

$$\Delta = \begin{pmatrix} -k_x\frac{\epsilon_{31}}{\epsilon_{33}} & -k_x\frac{\epsilon_{32}}{\epsilon_{33}} & 0 & 1-\frac{k_x^2}{\epsilon_{33}} \\ 0 & 0 & -1 & 0 \\ \epsilon_{23}\frac{\epsilon_{31}}{\epsilon_{33}} - \epsilon_{21} & k_x^2 - \epsilon_{22} + \epsilon_{23}\frac{\epsilon_{32}}{\epsilon_{33}} & 0 & k_x\frac{\epsilon_{23}}{\epsilon_{33}} \\ \epsilon_{11} - \epsilon_{13}\frac{\epsilon_{31}}{\epsilon_{33}} & \epsilon_{12} - \epsilon_{13}\frac{\epsilon_{32}}{\epsilon_{33}} & 0 & -k_x\frac{\epsilon_{13}}{\epsilon_{33}} \end{pmatrix}, \tag{161}$$

$$k_x \equiv n_a \sin\Phi_a. \tag{162}$$

The matrix now only depends on the dielectric function and on k_x. k_x comes from the x-component of the wave vector $\mathbf{k}$, which was assumed to be constant (since the medium only had z-dependence) when deriving Δ. What actually shows up in the derivation of Equation (148) is a factor $\frac{c}{\omega}\xi$ but with the use of Snell's law

$$\frac{c}{\omega}\xi = \frac{c}{\omega}k_b \sin\Phi_b = n_b \sin\Phi_b = n_a \sin\Phi_a \equiv k_x. \tag{163}$$

A further simplification can be made if the dielectric function ϵ has three principle axes, and the nine components comes from that the principle axes are rotated with respect to the laboratory frame. This can be expressed as

$$\boldsymbol{\epsilon} = \begin{pmatrix} \epsilon_{11} & \epsilon_{12} & \epsilon_{13} \\ \epsilon_{21} & \epsilon_{22} & \epsilon_{23} \\ \epsilon_{31} & \epsilon_{32} & \epsilon_{33} \end{pmatrix} = \mathbf{A} \begin{pmatrix} \epsilon_{0x} & 0 & 0 \\ 0 & \epsilon_{0y} & 0 \\ 0 & 0 & \epsilon_{0z} \end{pmatrix} \mathbf{A}^{-1}. \tag{164}$$

Here $\mathbf{A}$ is described by the three Euler angles $(\phi_E, \theta_E, \psi_E)$,

$$\mathbf{A}^T = \mathbf{A}^{-1} = \mathbf{R}(\phi_E, \theta_E, \psi_E) \tag{165}$$

$$= \begin{pmatrix} \cos\psi\cos\phi - \cos\theta\sin\phi\sin\psi & \cos\psi\sin\phi + \cos\theta\cos\phi\sin\psi & \sin\psi\sin\theta \\ -\sin\psi\cos\phi - \cos\theta\sin\phi\cos\psi & -\sin\psi\sin\phi + \cos\theta\cos\phi\cos\psi & \cos\psi\sin\theta \\ \sin\theta\sin\phi & -\sin\theta\cos\phi & \cos\theta \end{pmatrix} \tag{166}$$

which completely specify a rotation in three dimension, see for example Goldstein *et. al* [31]. Since $\mathbf{A}$ is orthogonal, $\mathbf{A}^{-1} = \mathbf{A}^T$ (since A is a rotation from one orthonormal coordinate system to another with determinant = 1). If the dielectric function have the form in Equation (164) then

$$\boldsymbol{\epsilon}^T = \left(\mathbf{A}\boldsymbol{\epsilon}_0\mathbf{A}^T\right)^T = \mathbf{A}\boldsymbol{\epsilon}_0^T\mathbf{A}^T = \mathbf{A}\boldsymbol{\epsilon}_0\mathbf{A}^T = \boldsymbol{\epsilon}. \tag{167}$$

Here $\boldsymbol{\epsilon}_0$ is the diagonal matrix in Equation (164). As a consequence, $\epsilon_{ij} = \epsilon_{ji}$ and there is nine unknowns, the real and complex part of the three principle dielectric constants and the three Euler angles. As mentioned above, this gives an exact form of the partial transfer matrix (with $\boldsymbol{\mu} = \mathbb{1}$ and $\boldsymbol{\rho} = \mathbb{0}$)[26]. But it is generally not true, since for a optical active media, $\boldsymbol{\epsilon}$ is hermitian ($\epsilon_{ij} = \epsilon_{ji}^*$)[10] and for a magnetic media, off-diagonal elements appears in the principle system.

3.4 Incident and exit matrix

By solving Equation (148), one gets the partial transfer matrices which says how (E_x, E_y, H_x, H_y) changes in the z-direction. But to see how s- and p-polarized light gets reflected and transmitted, the incident and exit matrix A_i^{-1} and A_f is also used. These matrices projects the s- and p-component of the incoming, reflected and transmitted light onto (E_x, E_y, H_x, H_y). They are defined as

$$A_i \begin{pmatrix} E_{is} \\ E_{rs} \\ E_{ip} \\ E_{rp} \end{pmatrix} = \begin{pmatrix} E_x \\ E_y \\ H_x \\ H_y \end{pmatrix}, \qquad A_f \begin{pmatrix} E_{ts} \\ 0 \\ E_{tp} \\ 0 \end{pmatrix} = \begin{pmatrix} E_x \\ E_y \\ H_x \\ H_y \end{pmatrix}. \tag{168}$$

Here it is assumed that there is no reflected wave in the substrate, an approximation that the substrate extend infinitely away from the material. This is reasonable since in experiment, substrate are chosen to be very thick. In the case of a isotropic ambient/substrate (ambient is the incoming medium, substrate outgoing), the procedure is rather straight forward. The $\mathbf{H}$- and $\mathbf{E}$ - fields are related through the Maxwell equation

$$\boldsymbol{\nabla} \times \mathbf{E} = -\frac{1}{c}\frac{\partial}{\partial t}\mathbf{H}, \tag{169}$$

$$\mathbf{k} \times \mathbf{E} = \frac{\omega}{c}\mathbf{H}. \tag{170}$$

Since $\mathbf{k}$, $\mathbf{E}$ and $\mathbf{H}$ are all orthogonal to eachother in an isotropic media, the following relation holds

$$|\mathbf{k}||\mathbf{E}| = n\frac{\omega}{c}|\mathbf{E}| = \frac{\omega}{c}|\mathbf{H}|, \tag{171}$$

$$nE = H. \tag{172}$$

This can be applied to both the p-polarized and s-polarized components. By simple geometry

$$A_i \begin{pmatrix} E_{is} \\ E_{rs} \\ E_{ip} \\ E_{rp} \end{pmatrix} = \begin{pmatrix} E_x \\ E_y \\ H_x \\ H_y \end{pmatrix} = \begin{pmatrix} E_{ip}\cos\theta_i \\ E_{is} \\ -n_i E_{is}\cos\theta_i \\ n_i E_{ip} \end{pmatrix} + \begin{pmatrix} -E_{rp}\cos\theta_i \\ E_{rs} \\ n_i E_{rs}\cos\theta_i \\ n_i E_{rp} \end{pmatrix}, \tag{173}$$

where the two vectors are the incident and reflected wave. From this equation, the inverse of the incident matrix becomes

$$A_i^{-1} = \frac{1}{2}\begin{pmatrix} 0 & 1 & -\frac{1}{n_i\cos\theta_i} & 0 \\ 0 & 1 & \frac{1}{n_i\cos\theta_i} & 0 \\ \frac{1}{\cos\theta_i} & 0 & 0 & \frac{1}{n_i} \\ -\frac{1}{\cos\theta_i} & 0 & 0 & \frac{1}{n_i} \end{pmatrix}. \tag{174}$$

Similarly for an isotropic substrate

$$A_f \begin{pmatrix} E_{ts} \\ 0 \\ E_{tp} \\ 0 \end{pmatrix} = \begin{pmatrix} E_x \\ E_y \\ H_x \\ H_y \end{pmatrix} = \begin{pmatrix} E_{tp}\cos\theta_t \\ E_{ts} \\ -n_t E_{ts}\cos\theta_t \\ n_t E_{tp} \end{pmatrix}, \tag{175}$$

resulting in

$$A_f = \begin{pmatrix} 0 & 0 & \cos\theta_t & 0 \\ 1 & 0 & 0 & 0 \\ -n_t\cos\theta_t & 0 & 0 & 0 \\ 0 & 0 & n_t & 0 \end{pmatrix}. \tag{176}$$

With Snell's law, which holds even if there is a medium inbetween the ambient and the substrate because of the symmetry of the problem, $\cos\theta_t = \sqrt{1-(\frac{n_i}{n_t}\sin\theta_i)^2}$. Here it is interesting to note that if there is no medium between the ambient and the substrate, the partial transfer matrix becomes

$$T_p(d) = e^{ik_0\Delta d} \xrightarrow[d\to 0]{} 1. \tag{177}$$

Equation (125) then becomes

$$\begin{pmatrix} E_{is} \\ E_{rs} \\ E_{ip} \\ E_{rp} \end{pmatrix} = T \begin{pmatrix} E_{ts} \\ 0 \\ E_{tp} \\ 0 \end{pmatrix} = A_i^{-1} A_f \begin{pmatrix} E_{ts} \\ 0 \\ E_{tp} \\ 0 \end{pmatrix} = \frac{1}{2}\begin{pmatrix} (1+\frac{n_t\cos\theta_t}{n_i\cos\theta_i})E_{ts} \\ (1-\frac{n_t\cos\theta_t}{n_i\cos\theta_i})E_{ts} \\ (\frac{\cos\theta_t}{\cos\theta_i}+\frac{n_t}{n_i})E_{tp} \\ (-\frac{\cos\theta_t}{\cos\theta_i}+\frac{n_t}{n_i})E_{tp} \end{pmatrix}. \tag{178}$$

The Fresnel's equations for reflection of p- respectively s-polarized light follows directly from this

$$r_s = \frac{E_{rs}}{E_{is}} = \frac{1 - n_t \cos\theta_t/(n_i \cos\theta_i}{1 + n_t \cos\theta_t/(n_i \cos\theta_i)} = \frac{n_i \cos\theta_i - n_t \cos\theta_t}{n_i \cos\theta_i + n_t \cos\theta_t}, \tag{179}$$

$$r_p = \frac{E_{rp}}{E_{ip}} = \frac{-\cos\theta_t/\cos\theta_i + n_t/n_i}{\cos\theta_t/\cos\theta_i + n_t/n_i} = \frac{n_t \cos\theta_i - n_i \cos\theta_t}{n_t \cos\theta_i + n_i \cos\theta_t}. \tag{180}$$

In the case of an anisotropic substrate, the complexity of the problem increases. However, experimentalists enjoy considerable freedom in selecting the substrate, which often leads to the utilization of a simple isotropic material for convenience. The solution is still covered here for completeness and one then has to solve the eigenvalue equation (Equation (153))

$$\Delta\psi_k = q_k \psi_k \tag{181}$$

and find the eigenvectors. Two of the eigenvalues will have a positive real part, which corresponds to transmitted waves, and two will have negative real parts, which then can be ignored because of the assumption of no reflected waves in the substrate. Assume the eigenvectors

$$\psi_a = \begin{pmatrix} \Xi_{1a} \\ \Xi_{2a} \\ \Xi_{3a} \\ \Xi_{4a} \end{pmatrix}, \qquad \psi_b = \begin{pmatrix} \Xi_{1b} \\ \Xi_{2b} \\ \Xi_{3b} \\ \Xi_{4b} \end{pmatrix}, \tag{182}$$

has positive eigenvalues. From these two transmitted eigenvectors, the exit matrix can be constructed:

$$A_f = \begin{pmatrix} \Xi_{1a} & 0 & \Xi_{1b} & 0 \\ \Xi_{2a} & 0 & \Xi_{2b} & 0 \\ \Xi_{3a} & 0 & \Xi_{3b} & 0 \\ \Xi_{4a} & 0 & \Xi_{4b} & 0 \end{pmatrix}. \tag{183}$$

3.5 Magneto-optical Measurements

When measuring spin-dynamics in materials, one generally look at how the intensity and the state of polarization change if incident light is reflected or transmitted. There are three types of measurements that can be done, either the rotation of polarization of the reflected light which is called the magneto-optic Kerr effect (MOKE), the rotation of polarization of transmitted light called Faraday rotation or one can look at the absorption of different polarization's. A weak external magnetic field is applied to the sample to align the spins making it possible to measure the spin-dynamics. The method developed here relies on the assumption that diagonal elements in the dielectric function is approximately the same and that the off diagonal elements other than $\epsilon_{12} = -\epsilon_{21}$ are negligible. This is often the case (e.g when there is cubic symmetry [19]) and the dielectric

function can then be written a simple form. For the polar configuration with magnetization perpendicular to the medium boundary it becomes

$$\boldsymbol{\epsilon} = N^2 \begin{pmatrix} 1 & iQ & 0 \\ -iQ & 1 & 0 \\ 0 & 0 & 1 \end{pmatrix}. \tag{184}$$

Here N is the refractive index, $N^2 = \epsilon_{xx}$ and $Q = -i\frac{\epsilon_{xy}}{\epsilon_{xx}}$ is called the magneto-optic constant, with the diagonal elements assumed to be equal. The quantities N and Q depend on the occupancy and vacancies of the electron states and can be theoretically calculated from DFT (see Section 2.8). These will have a frequency dependence because of resonances corresponding to excitations of the electrons. In the pump and probe measurements, which is explain in section (ref) , the sample will get excited from its ground state by a laser pulse and then relax back to the the ground state. During this period the dielectric function also has a time-dependence because of the transient dynamics.

3.6 Magneto-optic Approach

If the dielectric can be assumed to have the simplified form in Equation (184), one does not have to resort to the general differential approach to calculate the partial tranfer matrix. A universal approach for studying MOKE and surface magneto-optic Kerr effect (SMOKE) has been developed by J. Zak *et al.* [27] [28]. It is similar to the method that resulted in Equation (158), where the eigenvectors were found and the partial transfer matrix where expressed in terms of a product of the matrix composed of eigenvectors $\boldsymbol{\Psi}$ and the diagonal matrix $\mathbf{K}(d)$. J. Zak also uses 4×4 - matrices to transverse the electric and magnetic field components through the layered material, but he uses two different matrices. The first is a boundary matrix A defined as

$$\begin{pmatrix} E_x \\ E_y \\ H_x \\ H_y \end{pmatrix} = F = AP = A \begin{pmatrix} E_{si} \\ E_{pi} \\ E_{sr} \\ E_{pr} \end{pmatrix}, \tag{185}$$

which related the in-plane components of the E- and H- field with the s- and p-polarized incident and reflected beams. The second is a propagation matrix D which defines the propagation of rays from one boundary to another in a slab and relates the field amplitudes at the boundaries. D can either be chosen to propagate the eigenmodes or one that propagates the P vector above. The former would lead to a diagonal matrix similar to that of Equation (158). The dielectric function in Equation (184) is written in the polar configuration, which is when the magnetization is perpendicular to the sample surface and is called PMOKE.

For the longitudinal configuration (LMOKE), the magnetization is along the boundary and in the plane of incidence and the dielectric function then has the

form

$$\boldsymbol{\epsilon} = N^2 \begin{pmatrix} 1 & 0 & -iQ \\ 0 & 1 & 0 \\ iQ & 0 & 1 \end{pmatrix}. \tag{186}$$

This can then be generalized for arbitrary direction of magnetization, with the use of Euler angles writes the dielectric function as [28] [34]

$$\boldsymbol{\epsilon} = N^2 \begin{pmatrix} 1 & iQm_z & -iQm_y \\ -iQm_z & 1 & iQm_x \\ iQm_y & -iQm_x & 1 \end{pmatrix}. \tag{187}$$

Here m_i is the direction cosines of the magnetization vector. The direction cosines can be written in terms of the polar and azimuth angle (φ, γ) as

$$m_x = \sin\varphi\cos\gamma, \tag{188}$$
$$m_y = \sin\varphi\sin\gamma, \tag{189}$$
$$m_z = \cos\varphi. \tag{190}$$

The hardest task is to find the boundary matrix A which relates the partial waves inside the medium to the in-plane components at the boundary. To do this the propagation direction has to be found for the eigenmodes given the dielectric tensor. These are found from the Maxwell's equation by

$$\boldsymbol{\nabla} \times \mathbf{E} = i\mathbf{k} \times \mathbf{E} = -\frac{1}{c}\frac{\partial}{\partial t}\mathbf{H} = i\frac{\omega}{c}\mathbf{H} \tag{191}$$

$$\boldsymbol{\nabla} \times (\boldsymbol{\nabla} \times \mathbf{E}) = i^2\mathbf{k} \times (\mathbf{k} \times \mathbf{E}) = i\frac{\omega}{c}\boldsymbol{\nabla} \times \mathbf{H} = i\frac{\omega}{c^2}\frac{\partial}{\partial t}\mathbf{D} = \frac{\omega^2}{c^2}\mathbf{D} = k_0^2\boldsymbol{\epsilon}\mathbf{E} \tag{192}$$

$$\mathbf{k} \times (\mathbf{k} \times \mathbf{E}) = \mathbf{k}(\mathbf{k} \cdot \mathbf{E}) - k^2\mathbf{E} = -k_0^2\boldsymbol{\epsilon}\mathbf{E} \tag{193}$$

with $\mathbf{k} = \frac{\omega}{c}\mathbf{n}$,

$$n^2\mathbf{E} - \mathbf{n}(\mathbf{n} \cdot \mathbf{E}) - \boldsymbol{\epsilon}\mathbf{E} = \mathbf{0}. \tag{194}$$

This is a matrix equation with non-trivial solutions if

$$\det\big(n^2\delta_{ij} - n_i n_j - \epsilon_{ij}\big) = 0. \tag{195}$$

If the medium only has a z-dependence, then x- and y-component of the wave vector will stay constant. The equation above is quadratic in n_z which yields four roots. These correspond to the four eigenmodes, two that travels in positive and two in negative z-direction. [29].

Also, by finding the roots to the equation above gives the refractive index. One can assume $n_x = 0$ without loss of generality (it's just to define the y-axis

as being parallel to the plane of incidence). There is also four solutions to this equation, two rays in positive z-direction and two in the negative. For the polar case, to first order in Q, these are

$$n_{POL}^{(1,2)} = N(1 \pm \frac{1}{2}\alpha_z Q), \tag{196}$$

$$n_{POL}^{(3,4)} = N(1 \mp \frac{1}{2}\alpha_z Q), \tag{197}$$

with $\alpha_z = \cos\theta_j$. For the longitudinal configuration these are

$$n_{LON}^{(1,2)} = N(1 \pm \frac{1}{2}\alpha_y Q), \tag{198}$$

$$n_{LON}^{(3,4)} = N(1 \mp \frac{1}{2}\alpha_y Q), \tag{199}$$

with $\alpha_y = \sin\theta_j$. The four waves are denoted as $\mathbf{E}^{(1)}$, $\mathbf{E}^{(2)}$, $\mathbf{E}^{(3)}$ and $\mathbf{E}^{(4)}$. 1 and 2 are the two traveling in positive z-direction and 3 and 4 travels in the negative direction, with directions and refractive indexes given by the Equations (196 - 199). In order to find the boundary matrix A, the number of variables needs to be reduced. The components $E_x^{(j)}$, $E_y^{(j)}$ and $E_z^{(j)}$ for the four waves ($j = 1, ..., 4$) all satisfy the Fresnel equations and are thus dependent. It is then possible to express all components in terms of $E_x^{(j)}$. Further $H_x^{(j)}$ and $H_y^{(j)}$ needs to be expressed in terms of $\mathbf{P}$ and this can be done through the relation $\mathbf{H} = \mathbf{n} \times \mathbf{E}$. The derivation is rather cumbersome and is done by J. Zak in reference [27]. The final result for the boundary matrix A in the polar respectively longitudinal case are

$$A^{(POL)} = \begin{pmatrix} 1 & 0 & 1 & 0 \\ \frac{i}{2}\alpha_y^2 Q & \alpha_z & \frac{i}{2}\alpha_y^2 Q & -\alpha_z \\ \frac{i}{2}\alpha_z Q N & -N & -\frac{i}{2}\alpha_z Q N & -N \\ \alpha_z N & \frac{i}{2}QN & -\alpha_z N & \frac{i}{2}QN \end{pmatrix}, \tag{200}$$

$$A^{(LON)} = \begin{pmatrix} 1 & 0 & 1 & 0 \\ -\frac{i}{2}\frac{\alpha_y}{\alpha_z}(1+\alpha_z^2)Q & \alpha_z & \frac{i}{2}\frac{\alpha_y}{\alpha_z}(1+\alpha_z^2)Q & -\alpha_z \\ \frac{i}{2}\alpha_y Q N & -N & \frac{i}{2}\alpha_y Q N & -N \\ \alpha_z N & \frac{i}{2}\frac{\alpha_y}{\alpha_z}QN & -\alpha_z N & -\frac{i}{2}\frac{\alpha_y}{\alpha_z}QN \end{pmatrix}. \tag{201}$$

For a non-magnetic media, $Q = 0$ and the boundary matrix becomes

$$A = \begin{pmatrix} 1 & 0 & 1 & 0 \\ 0 & \alpha_z & 0 & -\alpha_z \\ 0 & -N & 0 & -N \\ \alpha_z N & 0 & -\alpha_z N & 0 \end{pmatrix} \tag{202}$$

What is left is to find the propagating matrix $\bar{D}$ which relates the P vector at the two boundaries. An eigenmode is related by

$$E_x^{(j)}(z = d) = E_x^{(j)}(z = 0)e^{i(\frac{\omega}{c}n^{(j)}\alpha_z^{(j)}d)}. \tag{203}$$

The P vector is related to the eigenmodes by

$$\begin{pmatrix} E_x^{(1)} \\ E_x^{(2)} \\ E_x^{(3)} \\ E_x^{(4)} \end{pmatrix} = \frac{1}{2} \begin{pmatrix} 1 & i & 0 & 0 \\ 1 & -i & 0 & 0 \\ 0 & 0 & 1 & \pm i \\ 0 & 0 & 1 & \mp i \end{pmatrix} \begin{pmatrix} E_s^{(i)} \\ E_p^{(i)} \\ E_s^{(r)} \\ E_p^{(r)} \end{pmatrix} = SP. \tag{204}$$

Thus the propagation matrix $\bar{D}$ can be written as

$$\bar{D} = S^{-1}DS = \begin{pmatrix} U\cos\sigma & U\sin\sigma & 0 & 0 \\ -U\sin\sigma & U\cos\sigma & 0 & 0 \\ 0 & 0 & U^{-1}\cos\sigma & \pm U^{-1}\sin\sigma \\ 0 & 0 & \mp U^{-1}\sin\sigma & U^{-1}\cos\sigma \end{pmatrix}. \tag{205}$$

Here the D matrix is the diagonal matrix with components given by Equation (203). $U = \exp(-i(2\pi/\lambda)N\alpha_z d)$ and the upper/lower signs are for the polar respectively longitudinal configuration. Finally

$$\sigma^{(POL)} = \frac{\pi}{\lambda} NQd, \tag{206}$$

$$\sigma^{(LON)} = \frac{\pi}{\lambda} NQd\frac{\alpha_y}{\alpha_z}. \tag{207}$$

For arbitrary magnetization direction in Equation 187, the boundary matrix for medium j can be written as

$$A_j = \begin{pmatrix} 1 & 0 & 1 & 0 \\ \frac{i}{2}\frac{\alpha_y}{\alpha_z}Q(\alpha_y g_i - 2m_x) & \alpha_z + i\alpha_y m_x Q & -\frac{i}{2}\frac{\alpha_y}{\alpha_z}Q(\alpha_y g_r - 2m_x) & -\alpha_z + i\alpha_y m_x Q \\ \frac{i}{2}Ng_i Q & -N & \frac{i}{2}Ng_r Q & -N \\ N\alpha_z & \frac{i}{2\alpha_z}Ng_i Q & -N\alpha_z & -\frac{i}{2\alpha_z}Ng_r Q \end{pmatrix}. \tag{208}$$

Here it's understood that $\alpha_z = \cos\theta_j$ and $\alpha_y = \sin\theta_j$ is given by the angle for medium j. It's easy to see that this reduces to the polar or longitudinal configuration with $m_z = 1$, $m_y = 0$ or $m_z = 0$, $m_y = 1$. The angles are determined by Snell's law $\sin\theta_j = \frac{N_{j-1}}{N_j}\sin\theta_{j-1}$ and $\cos\theta_j = (1 - \sin^2\theta_j)^{1/2}$ and

$$g_i = m_z\alpha_z + m_y\alpha_y, \tag{209}$$

$$g_r = -m_z\alpha_z + m_y\alpha_y. \tag{210}$$

The propagation matrix becomes

$$\bar{D}_j = \begin{pmatrix} U\cos\delta^i & U\sin\delta^i & 0 & 0 \\ -U\sin\delta^i & U\cos\delta^i & 0 & 0 \\ 0 & 0 & U^{-1}\cos\delta^r & U^{-1}\sin\delta^r \\ 0 & 0 & -U^{-1}\sin\delta^r & U^{-1}\cos\delta^r \end{pmatrix}, \tag{211}$$

where the components are defined as

$$U = \exp\left(-i\frac{2\pi}{\lambda}N\alpha_z d\right), \tag{212}$$

$$\delta^i = \frac{\pi}{\lambda}Nd\frac{Q}{\alpha_z}g_i, \tag{213}$$

$$\delta^r = \frac{\pi}{\lambda}Nd\frac{Q}{\alpha_z}g_r. \tag{214}$$

When the boundary and propagation matrices for all medium in the system has been calculated. The total transfer matrix can be calculated as follows (with $z = 0$ at the first boundary):

$$A_0P_0(z=0) = A_1P_1(0) = A_1\bar{D}_1(-d_1)P_1(d_1) = A_1\bar{D}_1A_1^{-1}A_1P_1(d_1) \tag{215}$$

$$= A_1\bar{D}_1A_1^{-1}A_2P_2(d_1) = A_1\bar{D}_1A_1^{-1}A_2\bar{D}_2A_2^{-1}A_3P_3 = ... \tag{216}$$

For N layers, and labeling $A_0P_0 = A_iP_i$ and $A_{N+1}P_{N+1} = A_fP_f$, the total expression becomes

$$P_i = A_i^{-1}\prod_{j=1}^{N}(A_j\bar{D}_j(-d_j)A_j^{-1})A_fP_f = TP_f, \tag{217}$$

with T similar to the total transfer matrix derived before.

4 Experiment

In the previous section, it was explained how the state of polarization changes when light is reflected on or transmitted through a sample. For reflection, it was shown how the Fresnel reflection matrix

$$\mathbf{R} = \begin{pmatrix}\tilde{r}_{pp} & \tilde{r}_{ps}\\ \tilde{r}_{sp} & \tilde{r}_{ss}\end{pmatrix}, \tag{218}$$

could be calculated from theory. Here the coefficients have been rewritten ($r \to \tilde{r}$) to distinguish them from their magnitude when written in polar form. In this section, a general experimental setup to measure this effect will be shown. The Jones matrix formalism will be used to represent the different optical elements and derive general expressions for the experimental setup that can be analyzed.

The first thing to understand is that the MOKE signal is very weak. This problem is usually resolved through modulator techniques where the incoming signal is given a certain frequency, which then can be used to distinguish the reflected signal from the noise. The signal to noise ratio is also effected by the relative orientations of the optical elements and there are some orientations and configurations that maximized the MOKE signal. This would be the signal caused by magnetization from the off-diagonal elements in the dielectric function, while minimizing the non-magnetic contribution from the diagonal ones [35][36].

4.1 Photo-elastic modulator (PEM)

A common optical element used for modulating the signal is a photo-elastic modulator (PEM). This is a material that has an optical axis with a refraction index that can be modulated by inducing a strain. An example of this is fused Silica which becomes birefringent under strain[9]. Then the ordinary and extra ordinary refractive index can be modulated by stretching or compressing the material. A piezoelectric transducer is then used, which mechanically oscillates with a certain frequency which gives rise to a frequency dependent polarization. The retardation angle can be written as $\varphi = \varphi_0 \sin(\omega_M t)$. The polarization after the PEM will then oscillate between RCP and LCP light with the frequency ω_M and a maximum phase retardation φ which both can be controlled. This frequency dependence can then be used in the lock-in amplifier to extract the reflected signal from the noise.

4.2 Experimental setup

A typical experimental setup for MOKE and surface MOKE (SMOKE) measurement is very similar. The difference is the transfer matrix needed in SMOKE because reflection and transmission trough the underlying substrate is needed [37]. There is a monochromatic light source (laser) that provides polarized light. The first optical element is a polarizer that prepares the light for the photo-elastic modulator (PEM). After the PEM, the light hits the sample and gets reflected. (PEM is before the sample in ref time-resolved magneto-optical measurements of ultrafast demagnitization, but after in reference [38]). The reflected light periodically modulated by the PEM between RCP and LCP to maximize the first and second harmonics of the Bessel functions in order to maximize the signal to noise ratio. The modulation signal is then used as a reference in the lock-in amplifier [38]. After the PEM the light is transmitted through an analyzer. Finally the signal hits a photosensitive diode which creates a signal that is proportional to the intensity which is then sent to the lock-in amplifier.

The experimental setup is easy to analyse with Jones matrix formalism. The linear polarized light from the light source can be written as

$$\mathbf{E}^i = \begin{pmatrix} E^i \\ 0 \end{pmatrix} = E^i \begin{pmatrix} 1 \\ 0 \end{pmatrix}. \tag{219}$$

The polarizer creates an equal polarization in the two polarization direction for the PEM

$$\mathbf{P} = \begin{pmatrix} \cos^2\theta_p & \sin\theta_a \cos\theta_p \\ \sin\theta_p \cos\theta_p & \sin^2\theta_p \end{pmatrix}. \tag{220}$$

For $\theta_p = 45°$

$$\mathbf{P} = \begin{pmatrix} \frac{1}{2} & \frac{1}{2} \\ \frac{1}{2} & \frac{1}{2} \end{pmatrix}. \tag{221}$$

The electric field components are now

$$\begin{pmatrix} E_{0p} \\ E_{0s} \end{pmatrix} = \mathbf{P}\mathbf{E}^i. \tag{222}$$

($E_{p0} = E_0 \cos\theta_p$ and $E_{s0} = E_0 \sin\theta_p$ in ref [37]) These are now modulated by the PEM (explained above) and are projected to the principle axis of the modulator

$$\mathbf{M}_0 = \begin{pmatrix} \cos\frac{\varphi}{2} - i\sin\frac{\varphi}{2}\cos(2\theta_m) & -i\sin\frac{\varphi}{2}\sin(2\theta_m) \\ -i\sin\frac{\varphi}{2}\sin(2\theta_m) & \cos\frac{\varphi}{2} + i\sin\frac{\varphi}{2}\cos(2\theta_m) \end{pmatrix} \tag{223}$$

θ_m is the angle of the principle axis of the modulator relative to the scattering plane (p-axis). This simplifies for special cases of θ_m. The three most common cases in MOKE experiments are

$$\mathbf{M}_0(\theta_m = 0) = \begin{pmatrix} e^{-i\varphi/2} & 0 \\ 0 & e^{i\varphi/2} \end{pmatrix}, \tag{224}$$

$$\mathbf{M}_0(\theta_m = \frac{\pi}{2}) = \begin{pmatrix} e^{i\varphi/2} & 0 \\ 0 & e^{-i\varphi/2} \end{pmatrix}, \tag{225}$$

$$\mathbf{M}_0(\theta_m = \frac{\pi}{4}) = \begin{pmatrix} \cos(\varphi/2) & -i\sin(\varphi/2) \\ -i\sin(\varphi/2) & \cos(\varphi/2) \end{pmatrix}. \tag{226}$$

After the PEM, the state of polarization is

$$\begin{pmatrix} E_i p \\ E_i s \end{pmatrix} = \mathbf{M_0} \begin{pmatrix} E_{0p} \\ E_{0s} \end{pmatrix}, \tag{227}$$

which is the light that is incident on the sample. The reflected light from the sample is given by

$$\begin{pmatrix} E_{rp} \\ E_{rs} \end{pmatrix} = \mathbf{R} \begin{pmatrix} E_{ip} \\ E_{is} \end{pmatrix}. \tag{228}$$

Here $\mathbf{R}$ is the Fresnel reflection matrix

$$\mathbf{R} = \begin{pmatrix} \tilde{r}_{pp} & \tilde{r}_{ps} \\ \tilde{r}_{sp} & \tilde{r}_{ss} \end{pmatrix}, \tag{229}$$

which elements calculated from the methods mention in previous sections. Finally there is an analyzer before the signal hits the photodiode at an angle θ_a which can be represented by the matrix

$$\mathbf{A} = \begin{pmatrix} \cos^2\theta_a & \sin\theta_a\cos\theta_a \\ \sin\theta_a\cos\theta_a & \sin^2\theta_a \end{pmatrix}. \tag{230}$$

The final measured signal is then given by

$$\mathbf{E}^r = \mathbf{A}\mathbf{R}\mathbf{M}_0\mathbf{P}\mathbf{E}^i \tag{231}$$

To calculate the intensity $|\mathbf{E}|^2 = |E_x|^2 + |E_y|^2$ in the Jones formalism, one simple multiply the polarization vector by the conjugate transpose

$$|\mathbf{E}|^2 = \mathbf{E}^\dagger \mathbf{E} = \begin{pmatrix} E_x^* & E_y^* \end{pmatrix} \begin{pmatrix} E_x \\ E_y \end{pmatrix} = |E_x|^2 + |E_y|^2. \tag{232}$$

The reflected intensity can then be calculated similarly

$$I^r = (\mathbf{E}^r)^\dagger \mathbf{E}^r = \left|E^i\right|^2 \begin{pmatrix} 1 & 0 \end{pmatrix} \mathbf{P}^\dagger \mathbf{M}_0^\dagger \mathbf{R}^\dagger \mathbf{A}^\dagger \mathbf{A} \mathbf{M}_0 \mathbf{R} \mathbf{P} \begin{pmatrix} 1 \\ 0 \end{pmatrix} \tag{233}$$

$$= \tilde{I} \frac{\left|E^i\right|^2}{2} = \tilde{I} \frac{I^i}{2}. \tag{234}$$

Following reference [9] with $\theta_m = \frac{\pi}{2}$, $\tilde{I}$ can be written as a sum of three terms

$$\tilde{I} = A + B\cos\varphi + C\sin\varphi, \tag{235}$$

with factors given by

$$A = r_p^2 \cos^2\theta_a + r_s^2 \sin^2\theta_a \tag{236}$$

$$+ r_{sp}^2 + r_{sp}\sin(2\theta_a)(r_p\cos(\delta_p - \delta_{sp}) - r_s\cos(\delta_s - \delta_{sp})), \tag{237}$$

$$B = \sin(2\theta_a)(r_s r_p \cos(\delta_p - \delta_s) - r_{sp}^2) \tag{238}$$

$$+ 2r_{sp}(r_s \sin^2\theta_a \cos(\delta_s - \delta_{sp}) 0 \cos^2\theta_a \cos(\delta_p - \delta_{sp})), \tag{239}$$

$$C = r_s r_p \sin(2\theta_a)\sin(\delta_s - \delta_p) \tag{240}$$

$$+ 2r_{sp}(r_s \sin^2\theta_a \sin(\delta_s - \delta_{sp}) + r_p \cos^2\theta_a \sin(\delta_p - \delta_{sp})). \tag{241}$$

To get these expressions, it was assumed that $\tilde{r}_{sp} = -\tilde{r}_{ps}$ for symmetry reasons and the complex reflection coefficients was expressed in their polar form

$$\tilde{r}_A = r_a e^{i\delta_A}, \tag{242}$$

with $A = p, s, sp, ps$. Since $\varphi = \varphi_0 \sin(\omega_M t)$, cos and sin can be expanded with the Bessel functions J_k:

$$\sin(\varphi_0 \sin(\omega_M t)) = J_1(\varphi_0)\sin(\omega_M t) + 2J_3(\varphi_0)\sin(3\omega_M t) + ... \tag{243}$$

$$\cos(\varphi_0 \sin(\omega_M t)) = J_0(\varphi_0)\sin(\omega_M t) + 2J_2(\varphi_0)\sin(2\omega_M t) + ... \tag{244}$$

If only terms up to the second harmonic is kept Equation (235) can be written as

$$\tilde{I} = \tilde{I}_0 + \tilde{I}_\omega \sin(\omega_M t) + \tilde{I}_{2\omega}\cos(2\omega_M t). \tag{245}$$

Here

$$\tilde{I}_0 = A + BJ_0(\varphi_0), \tag{246}$$

$$\tilde{I}_\omega = 2CJ_1(\vartheta_0), \tag{247}$$

$$\tilde{I}_{2\omega} = 2BJ_2(\vartheta_0). \tag{248}$$

$$\tag{249}$$

From the first and second harmonics, it is possible to find a relation to the Kerr ellipticity and Kerr rotation in the complex Kerr rotation. For normal incident light, with PEM phase $\varphi \approx 2.41$ which makes $J_0(\varphi) \approx 0$ and with $r_{sp}^2 \ll r^2$, M. Giovannella *et al.* [9] showed that first harmonic is proportional to the Kerr ellipticity and the second harmonic is proportional to the Kerr rotation:

$$\frac{\tilde{I}_\omega}{\tilde{I}_0} = -4J_1(\varphi_0)\epsilon_k^s, \tag{250}$$

$$\frac{\tilde{I}_{2\omega}}{\tilde{I}_0} = 2J_2(\varphi)\frac{\sin^2(2\theta_a)}{r} - 4J_2(\varphi)\cos(2\theta_a)\theta_k^s. \tag{251}$$

θ_k^s and ϵ_k^s are the real and imaginary part of the complex Kerr rotation defined in Equation (50). This information is then used the lock-in amplifier to extract the signal from the noise.

4.3 Asymmetry measurement

It is not always convenient to measure the complex Kerr rotation. Above, the incoming light was right and left circular polarized, which is used for many MOKE experiments in the optical region. But if one want to study transitions from the core electrons, the energies need to be in the x-ray regime (30-100eV for M-edge). Since there is harder to produce circular polarized light at these energies, people often resort to linear polarized light instead. Then TMOKE is commonly used and the magnetization can be measured by the asymmetry parameter A defined as [39]

$$A = \frac{I_p^+ - I_p^-}{I_p^+ + I_p^-} \approx 2\,\mathrm{Re}\left\{\frac{\sin(2\theta_i)\epsilon_{xy}}{N^4\cos^2\theta_i - N^2 + \sin^2\theta_i}\right\}, \tag{252}$$

with the assumption that ϵxy is small compared to N and thus second order terms be neglected. The reflected intensities for p-polarized light are

$$I_\pm^p = I_0\left|\frac{N\cos\theta_i - \cos\theta_t}{N\cos\theta_i + \cos\theta_t} \pm \frac{2\sin\theta_i\cos\theta_i}{N^2(N\cos\theta_i + \cos\theta_t)^2}\epsilon_{xy}\right|^2. \tag{253}$$

The $\pm$ stands for the direction of magnetization. For s-polarized light the reflected intensity is simply

$$I^s = I_0\left|\frac{\cos\theta_i - N\cos\theta_t}{\cos\theta_i + N\cos\theta_t}\right|^2. \tag{254}$$

This expression is derived from solving Maxwell's equations for a single boundary [40]. It is then often assumed that ϵ_{xy} is linearly proportional to the magnetization, hence also the asymmetry parameter. There has been doubts about a simple relationship [18], and even recently by S. Jana *et al* [41] has reported concerns about such a simple relationship in pump-probe measurements. They used what they call a magnetization-asymmetry test ratio (MAT ratio). I will

calculate the asymmetry parameter numerically with the matrix method where internal reflections are considered as well, to see how valid the approximation in Equation (252) is. Then the asymmetry parameter was calculated as

$$A = \frac{\left|r_{ps}^{+} + r_{pp}^{+}\right|^2 - \left|r_{ps}^{-} + r_{pp}^{-}\right|^2}{\left|r_{ps}^{+} + r_{pp}^{+}\right|^2 + \left|r_{ps}^{-} + r_{pp}^{-}\right|^2}, \tag{255}$$

where r_{ij} are the reflection coefficients in Fresnels reflection matrix (Equation (138)).

5 Result

The boundary and propagation matrix defined in Equation (208) and (211) was used to numerically calculate the total transfer matrix 217 from where Fresnel reflection matrix 138 was derived. From this matrix, various measurable quantities could be calculated. As a test for the method the result presented by J. Zak[28] was reproduced in Figure 8 with very good agreement. The same Python code was then used to analyze more realistic problems, where a dielectric function $\epsilon = \epsilon(E)$ was calculated by M. Elhanoty with DFT.

For the comparison, the complex Kerr rotation (Equation (50)) is plotted against the angle of incidence for six different magnetization directions (φ) and three different setups. These setups are from right to left; bulk Fe (single boundary), 50Å Fe on Au substrate and 50 stacked bilayers of 10Å Fe/10Å Au on Au substrate. The ambient in all three cases is air with $N = 1$ and the wavelength used was that from a He-Ne laser with $\lambda = 6328\mathring{A}$. Refractive indices and magneto-optic constants for Fe and Au was taken from the paper as

$$\begin{aligned} \text{Fe:} \quad & N = 2.87 + i3.36, \\ & Q = 0.0376 + i0.0066, \\ \text{Au:} \quad & N = 0.12 + i3.29, \\ & Q = 0. \end{aligned}$$

The plots shows how the signal changes significantly and the peaks gets shifted as both the angle of incident θ_i and magnetization direction φ is changed, which illustrates the power of the method to predict optimal experimental setups.

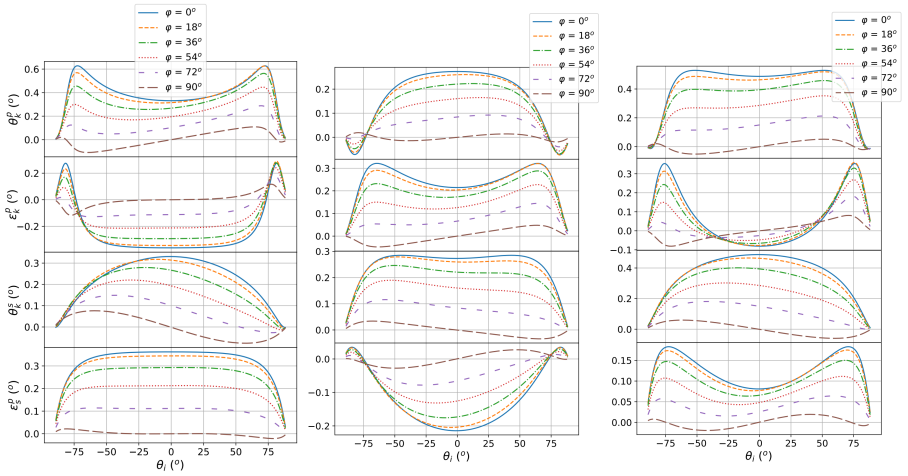

Figure 8: Complex Kerr rotation $\vartheta_k = \theta_k + i\epsilon_k$ plotted against angle of incidence θ_i for s- and p-polarized light. It also shows the signal for six different magnetization directions φ. The figures from left to right is for: Bulk Fe, 50Å Fe on Au substrate, 50 bilayers of 10Å Fe/ 10Å Au on Au substrate. These results agree very well with reference [28].

The asymmetry parameter $A = (I_+^p - I_-^p)/(I_+^p + I_-^p)$ in Equation (255) was calculated for the setup (2nm MgO)-(20nm Ni)-SiO for different angles of incidence. The result in the energy range 33-87 eV are shown in Figure 9 and the energy range 55-70eV in Figure 10. The four plots in each figure shows how the signal is differ when the different layers are taken into consideration to test the assumption for the asymmetry parameter in Equation (252). This calculation was done with the magneto-optic approach outlined in Section 3.6 with the dielectric function on the form in Equation (184).

The nine components of the dielectric function for Ni was calculated from DFT which are shown in Figure 11. Here it is clear that the simplified form is a valid assumption in the energy range 55-70eV, since $\epsilon_{12} \approx -\epsilon_{21}$, $\epsilon_{11} = \epsilon_{22} = \epsilon_{33}$ and $|\epsilon_{11}| > |\epsilon_{12}| \gg |\epsilon_{13}|, |\epsilon_{23}|, |\epsilon_{31}|, |\epsilon_{32}|$. The refractive index of MgO taken from reference [42] and SiO from reference [43]. (All found first from filmetrics.com) At these places they are given as a function of energy, but an average on the relevant energy range was chosen for simplicity since the focus is how signal changes when the layers are taken into consideration and the angular dependence, not the exact position of the peaks. This could however easily be implemented. The refractive indices used was

$$\begin{aligned} \text{MgO:} \qquad & N = 1.73, \\ \text{SiO:} \qquad & N = 1.7369 + i0.84315. \end{aligned}$$

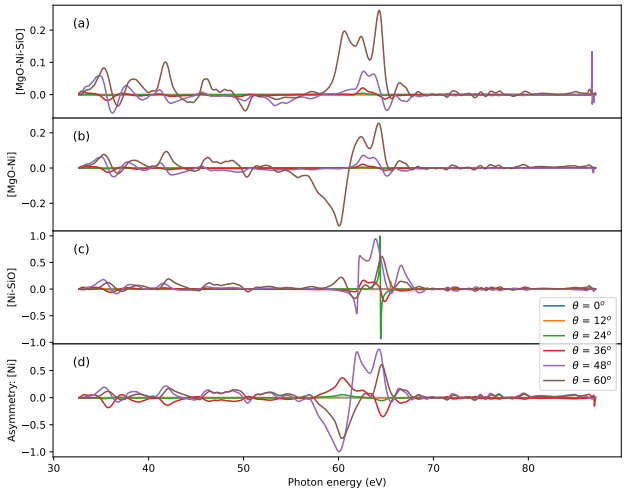

Figure 9: Calculated energy dependence of the asymmetry parameter A for different angles of incidence. The experimental setup was (2nm MgO)-(20nm Ni)-SiO and different layers where taken into consideration in the four plots.

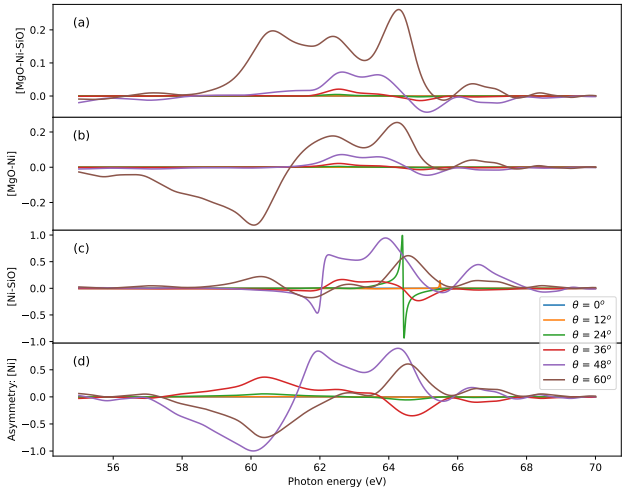

Figure 10: Here the region of interest in Figure 9 are shown.

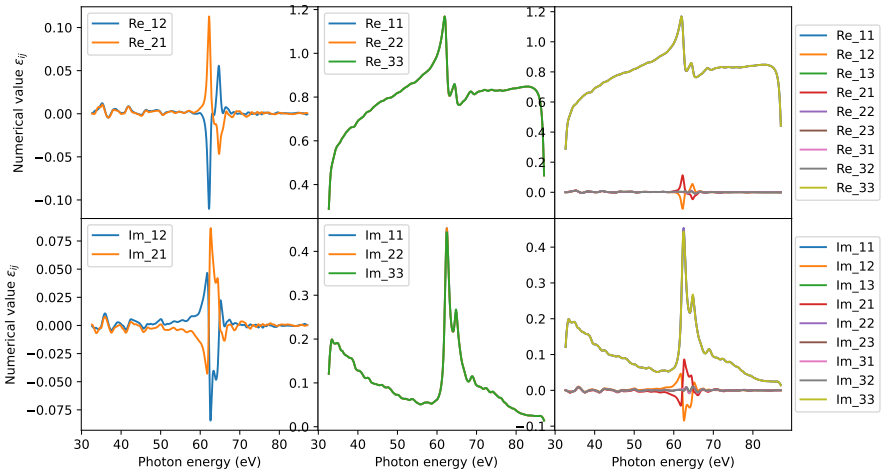

Figure 11: The real and imaginary parts of the nine components in the dielectric function for Ni are compared.

6 Discussion

Magnetization dynamics is an active field of research with promising future prospect where many aspects of physics comes together. In this paper the connection between the quantum mechanical and macroscopic world has been made through Maxwell's equations and the dielectric function. A brief overview on the theoretical background to understand a magneto-optic experiment has been done. The phenomenological question "What is going on?" has tried to be answered in simple terms and concrete methods of calculation which are used by the scientific community has been reviewed. Then the experimental techniques to measure MO effects was discussed and their connection to theory were made.

The main part has been devoted to a general transfer matrix method to relate theoretical calculations to measurable optical quantities such as the Fresnels reflection and transmission matrix. These matrices tells you how much s- and p-polarized light gets reflected and transmitted for a given experimental setup, which in turn can be related to the state of magnetization in a material. The matrix method was divided in two parts, which I called the differential and magneto-optic approach, the later gives analytic expressions to first order in Q for the matrices but requires three conditions to be met.

The magneto-optic approach outlined in Section 3.6 has been implemented in Python with good success. Even though only a handful of results has been presented, the written code can handle arbitrary layered systems and parameters such as photon energy, angle of incidence, magnetization direction, layer thicknesses, refractive indices and magneto-optic constants can be varied.

The result presented by J. Zak in his paper[28] was reproduced with excellent agreement in Figure 8. The same code was then used to calculate the asymmetry parameter in Figure 9 and 10 for a typical experimental setup in a pump and probe experiment. This result shows the complications in predicting a signal due to interference of multiple reflections and cast doubts on the validity in the simplified expression for the asymmetry parameter 252 used in the literature [39][40]. The result also illustrates the power of the method in predicting geometries that maximizes the signal. Changing the angle of incidence by just 12° can change the signal dramatically and the optimal angle depends both on the layers and photon energy.

By talking with experimentalists at Uppsala University, it has come to my attention that it is not clear what signal to expect when designing an experiment for a new material. Often the choice of energies and geometry are somewhat arbitrary and it is then case of trial and error, which is a time consuming process. If one instead adapt the transfer matrix method, one can with the help of first principle calculations get a hint on what signal to expect and the optimal geometry to maximize the signal to noise. The later is of crucial importance since the magneto optic effects are small.

The experimental setup used for the result in Figure 10 is from an actual pump probe experiment, but because of time constraints the values was never compared to experimental results. This holds true for all other calculations as

well and is the main concern regarding the results. The result in Figure 8 was in exceptional agreement with Ref. [28], with the curves for bulk Fe reported to be in a full qualitative agreement with published result in Ref. [44]. But this is for a single boundary and it would be valuable with experimental confirmation of multiple layered media to see how good the method is for predicting results and the validity of the approximations that goes into the magneto-optic approach.

In the event that the approximation is deemed invalid, it would be necessary to rely on the general differential approach to calculate the partial transfer matrix. Python implementation of this method has not been developed and is another area of improvement. If this is done, values from the two methods could be compared to better understand the criterion necessary for applying the magneto-optic approach, which is preferable since it is less computational demanding.

7 Outlook

There are numerous path available to pursue further research in this field and build upon the work presented here. The first obvious step would be to implement the more general differential matrix approach in code to compare with the other one, since all the necessary equations has already been derived. This was never done because of time limitations, but would both make it possible to confirm the validity of the differential approach and the approximations going into the magneto-optic one. The approximate form of the dielectric function in Equation (184), with Q small compared to N, ($\epsilon_{xy} << \epsilon_{xx}$), allowed for the latter. This assumption was tested for Ni in the sense that the sizes of each matrix element was compared, but a comparison between the two methods with actual calculations could confirm this assumption. With an implementation of the differential approach, materials with a dielectric function of more complicated form could be also tested and higher order contributions could be investigated.

This leads to the second point that could be worked on which is the requirements for the magneto-optic approach, namely the assumptions that permeability $\mu = 1$, gyrotropic matrix $\rho = 0$ and the higher order terms of Q is small. An investigation on what mechanisms give rise to these effects and require them to be considered for the mechanism to be observable would be interesting.

Symmetry arguments that specifies the form of the dielectric function is another thing that would be both interesting and fruitful to explore. It was mentioned that cubic symmetry give rise to the form necessary for the magneto-optic approach, but a detailed study could give valuable information on which elements in the dielectric function is most prevalent.

Lastly, a collaboration with experimentalists would be great. Then information about what specific measurements they do and are able to do could be used both when choosing the observable quantities that is calculated and when determining which parameters to vary when analysing the setup. The analysis could also be deepened by taking the other optical elements in the experimental setup into consideration with the Jones formalism similar to what was done in

Section 4.2. This could give a more complete picture and greater accuracy in predicting the measured signal and the possibility to optimize setup as a whole. Because of the many parameters involved in an experiment, this would be best done together with an experimental group but it could also be done for a general experiment.

8 Conclusions

A general matrix formalism has been derived to solve optical problems for layered magnetic media of arbitrary geometry. Depending on the form of the dielectric function, two approaches to calculate the partial transfer matrix for a layer has been presented. One of them was implemented in Python and compared to earlier results with excellent agreement. It was then used to calculate the asymmetry parameter which is frequently used in the literature as a measure of magnetization in a material. The results show that the signal vary significantly when different layers in an experimental setup is taken into consideration which illustrates the advantage in implementing this technique, not only to compare theory with experiment but also predicting an optimal experimental setup to maximize signal to noise.

References

1. Jones N. How to stop data centres from gobbling up the world's electricity. eng. Nature (London) 2018; 561:163–6
2. Li X and Yang J. First-principles design of spintronics materials. National Science Review 2016 Sep; 3:365–81. DOI: 10.1093/nsr/nww026
3. Premasiri K and Gao XPA. Tuning spin-orbit coupling in 2D materials for spintronics: a topical review. Journal of Physics-Condensed Matter 2019 May; 31. DOI: 10.1088/1361-648X/ab04c7
4. Bandyopadhyay S and Cahay M. Electron spin for classical information processing: a brief survey of spin-based logic devices, gates and circuits. Nanotechnology 2009 Oct; 20. DOI: 10.1088/0957-4484/20/41/412001
5. Hylick A, Sohan R, Rice A, and Jones B. An Analysis of Hard Drive Energy Consumption. eng. *2008 IEEE International Symposium on Modeling, Analysis and Simulation of Computers and Telecommunication Systems*. IEEE, 2008 :1–10
6. Griffiths DJ. Introduction to electrodynamics. Cambridge University Press, 2017
7. Dresselhaus MS, Dresselhaus G, Cronin SB, and Souza FAG. Solid state properties: From bulk to Nano. Springer, 2018
8. Landau L and Lifshitz E. Electrodynamics of Continous Media. 2nd ed. Vol. 8. Elsevier, 1984
9. Giovannella M, Eisebitt S, and Korff Schmising C von. Time resolved magneto-optical measurements of ultrafast demagnetization dynamics. PhD thesis. Tesi di laurea magistrale, Universita degli Studi di Pisa, 2013
10. Stone JM. Radiation and optics: An introduction to the classical theory. McGraw-Hill, 1963
11. Stöhr J and Siegmann HC. Magnetism: From Fundamentals to Nanoscale Dynamics. eng. 1. Aufl. Vol. 152. Springer series in solid-state sciences. Berlin, Heidelberg: Springer-Verlag, 2006
12. Beaurepaire E, Merle J, Daunois A, and Bigot J. Ultrafast spin dynamics in ferromagnetic nickel. eng. Physical review letters 1996; 76:4250–3
13. Sato K and Ishibashi T. Fundamentals of Magneto-Optical Spectroscopy. FRONTIERS IN PHYSICS 2022 Oct; 10. DOI: 10.3389/fphy.2022.946515
14. Nakamura J, Liang S, Gardner GC, and Manfra MJ. Direct observation of anyonic braiding statistics. Nature Physics 2020 Sep; 16:931+. DOI: 10.1038/s41567-020-1019-1
15. Griffiths DJ. Introduction to quantum mechanics. eng. Third edition. Cambridge, United Kingdom: Cambridge University Press, 2018

16. Kittel Charles 1. Introduction to solid state physics. eng. 7. ed. New York: Wiley, 1996

17. Argyres PN. Theory of the Faraday and Kerr Effects in Ferromagnetics. Phys. Rev. 1955 Jan; 97(2):334–45. DOI: 10.1103/PhysRev.97.334. Available from: https://link.aps.org/doi/10.1103/PhysRev.97.334

18. Misemer D. The effect of spin-orbit interaction and exchange splitting on magneto-optic coefficients. eng. Journal of magnetism and magnetic materials 1988; 72:267–74

19. Bennett HS and Stern EA. Faraday Effect in Solids. eng. Physical review 1965; 137:A448–A461

20. Sakurai JJ. Modern Quantum Mechanics. eng. Third edition. Cambridge: Cambridge University Press, 2021

21. Oppeneer PM, Maurer T, Sticht J, and Kubler J. Ab initio calculated magneto-optical Kerr effect of ferromagnetic metals : Fe and Ni. eng. Physical review. B, Condensed matter 1992; 45:10924–33

22. Elhanoty MF. Laser induced ultrafast magnetization dynamics studied with ab initio methods. PhD thesis. Uppsala University, 2022

23. Sholl DS. Density functional theory a practical introduction. eng. Hoboken, N.J: Wiley, 2009

24. Jones RC. A New Calculus for the Treatment of Optical SystemsI Description and Discussion of the Calculus. Journal of the Optical society of America. 1941-07-01; 31:488–93

25. Florin A. La théorie générale des couches minces (The generalized theory of thin films). Journal de Physique et le Radium 1950; 11:307–9. DOI: 10.1051/jphysrad:01950001107030700

26. Schubert M. Polarization-dependent optical parameters of arbitrarily anisotropic homogeneous layered systems. Phys. Rev. B 1996 Feb; 53(8):4265–74. DOI: 10.1103/PhysRevB.53.4265. Available from: https://link.aps.org/doi/10.1103/PhysRevB.53.4265

27. Zak J, Moog E, Liu C, and Bader S. Universal approach to magneto-optics. eng. Journal of magnetism and magnetic materials 1990; 89:107–23

28. Zak J, Moog ER, Liu C, and Bader SD. Magneto-optics of multilayers with arbitrary magnetization directions. eng. Physical review. B, Condensed matter 1991; 43:6423–9

29. Yeh P. Optics of anisotropic layered media: A new 4 × 4 matrix algebra. eng. Surface science 1980; 96:41–53

30. Fujiwara H. Spectroscopic ellipsometry: Principles and applications. John Wiley and Sons, 2007

31. Goldstein H, Poole C, and Safko J. Classical mechanics. Pearson, 2014

32. Berreman DW. Optics in Stratified and Anisotropic Media: 4×4-Matrix Formulation. Journal of the Optical society of America. 1972-04-01; 62:502

33. Wohler H, Haas G, Fritsch M, and Mlynski D. Faster 4x4 Matrix-Method for Uniaxial Inhomogeneous-Media. Journal of the Optical Society of America A-Optics Image Science and Vision 1988 Sep; 5:1554–7. DOI: 10.1364/JOSAA.5.001554

34. You CY and Shin SC. Generalized analytic formulae for magneto-optical Kerr effects. eng. Journal of applied physics 1998; 84:541–6

35. Polisetty S, Scheffler J, Sahoo S, Wang Y, Mukherjee T, He X, and Binek C. Optimization of magneto-optical Kerr setup: Analyzing experimental assemblies using Jones matrix formalism. eng. Review of scientific instruments 2008; 79:055107-055107–6

36. Légaré K, Chardonnet V, Bermúdez Macias I, Hennes M, Delaunay R, Lassonde P, Légaré F, Lambert G, Jal E, and Vodungbo B. Analytic description and optimization of magneto-optical Kerr setups with photoelastic modulation. eng. Review of scientific instruments 2022; 93:73001–1

37. Yang ZJ and Scheinfein MR. Combined three-axis surface magneto-optical Kerr effects in the study of surface and ultrathin-film magnetism. Journal of Applied Physics 1993; 74:6810–23. DOI: 10.1063/1.355081. eprint: https://doi.org/10.1063/1.355081. Available from: https://doi.org/10.1063/1.355081

38. Polisetty S, Scheffler J, Sahoo S, Wang Y, Mukherjee T, He X, and Binek C. Optimization of magneto-optical Kerr setup: Analyzing experimental assemblies using Jones matrix formalism. Review of Scientific Instruments 2008 May; 79. DOI: 10.1063/1.2932445

39. Mathias S, La-o-vorakiat C, Shaw JM, Turgut E, Grychtol P, Adam R, Rudolf D, Nembach HT, Silva TJ, Aeschlimann M, Schneider CM, Kapteyn HC, and Murnane MM. Ultrafast element-specific magnetization dynamics of complex magnetic materials on a table-top. Journal of Electron Spectroscopy and Related Phenomena 2013 Aug; 189:164–70. DOI: 10.1016/j.elspec.2012.11.013

40. Höchst H, Rioux D, Zhao D, and Huber DL. Magnetic linear dichroism effects in reflection spectroscopy: A case study at the Fe M2,3 edge. Journal of Applied Physics 1997 Jun; 81:7584–8. DOI: 10.1063/1.365303. eprint: https://pubs.aip.org/aip/jap/article-pdf/81/11/7584/10582255/7584_1_online.pdf. Available from: https://doi.org/10.1063/1.365303

41. Jana S, Malik RS, Kvashnin YO, Locht ILM, Knut R, Stefanuik R, Di Marco I, Yaresko AN, Ahlberg M, Akerman J, Chimata R, Battiato M, Soderstrom J, Eriksson O, and Karis O. Analysis of the linear relationship between asymmetry and magnetic moment at the M edge of 3d transition metals. Physical Review Research 2020 Feb; 2. DOI: 10.1103/PhysRevResearch.2.013180

42. Bass M. Handbook of Optics: Vol. 4, Set: Optical Properties of Materials, Nonlinear Optics, Quantum Optics. eng. 3rd ed. / Michael Bass, editor in chief. McGraw-Hill's AccessEngineering. Place of publication not identified: McGraw Hill Professional Publishing, 2009

43. Philipp H. Optical properties of non-crystalline Si, SiO, SiOx and SiO2. eng. The Journal of physics and chemistry of solids 1971; 32:1935–45

44. Metzget G, Plubinag.P, and Torguet R. Termes Lineaires et Quadratiques dans Leffet Magneto-optique de Kerr. Annales de Physique 1965; 10:5–&

9 Appendix

9.1 Matrix elements for Δ

The components in the Δ-matrix in Equation (148)

$$\begin{aligned}
\Delta_{11} &= M_{51} + (M_{53} + c\xi/\omega)a_{31} + M_{56}a_{61}, \\
\Delta_{12} &= M_{55} + (M_{53} + c\xi/\omega)a_{35} + M_{56}a_{65}, \\
\Delta_{13} &= M_{52} + (M_{53} + c\xi/\omega)a_{32} + M_{56}a_{62}, \\
-\Delta_{14} &= M_{54} + (M_{53} + c\xi/\omega)a_{34} + M_{56}a_{64}, \\
\Delta_{21} &= M_{11} + M_{13}a_{31} + M_{16}a_{61}, \\
\Delta_{22} &= M_{15} + M_{13}a_{35} + M_{16}a_{65}, \\
\Delta_{23} &= M_{12} + M_{13}a_{32} + M_{16}a_{62}, \\
-\Delta_{24} &= M_{14} + M_{13}a_{34} + M_{16}a_{64}, \\
-\Delta_{31} &= M_{41} + M_{43}a_{31} + M_{46}a_{61}, \\
-\Delta_{32} &= M_{45} + M_{43}a_{35} + M_{46}a_{65}, \\
-\Delta_{33} &= M_{42} + M_{43}a_{32} + M_{46}a_{62}, \\
\Delta_{34} &= M_{44} + M_{43}a_{34} + M_{46}a_{64}, \\
\Delta_{41} &= M_{21} + M_{23}a_{31} + (M_{26} - c\xi/\omega)a_{61}, \\
\Delta_{42} &= M_{25} + M_{23}a_{35} + (M_{26} - c\xi/\omega)a_{65}, \\
\Delta_{43} &= M_{22} + M_{23}a_{32} + (M_{26} - c\xi/\omega)a_{62}, \\
-\Delta_{44} &= M_{24} + M_{23}a_{34} + (M_{26} - c\xi/\omega)a_{64},
\end{aligned}$$

where M_{ij} are the elements in the M-matrix given by Equation (143). The a_{ij}'s are

$$\begin{aligned}
a_{31} &= (M_{61}M_{36} - M_{31}M_{66})/d, \\
a_{32} &= ((M_{62} - c\xi/\omega)M_{36} - M_{32}M_{66})/d, \\
a_{34} &= (M_{64}M_{36} - M_{34}M_{66})/d, \\
a_{35} &= (M_{65}M_{36} - (M_{35} + c\xi/\omega)M_{66})/d, \\
a_{61} &= (M_{63}M_{31} - M_{33}M_{61})/d, \\
a_{62} &= (M_{63}M_{32} - M_{33}(M_{62} - c\xi/\omega))/d, \\
a_{64} &= (M_{63}M_{34} - M_{33}M_{64})/d, \\
a_{65} &= (M_{63}(M_{35} + c\xi/\omega) - M_{33}M_{65})/d,
\end{aligned}$$

with

$$d = M_{33}M_{66} - M_{36}M_{63}.$$

9.2 Code

Code based on the magneto-optic approach which calculates the general transfer matrix and Fresnel's reflection and transmission matrix.

```
import numpy as np
import matplotlib.pyplot as plt
from numpy.linalg import inv
import itertools

#Creates a boundary matrix, for a medium of with magnetp-optical
    constant Q
#magnitization direction given by M, refractive intex n
#alpha_y = sintheta, alpha_z = costheta, theta from snells law
def boundarymatrix(Q,M,alpha_y, alpha_z,n):
    m_x = M[0]
    m_y = M[1]
    m_z = M[2]
    g_i = m_z*alpha_z + alpha_y*m_y
    g_r = -m_z*alpha_z + alpha_y*m_y
    return np.array([[1, 0, 1, 0],
                     [1j*alpha_y*Q/(2*alpha_z)*(alpha_y*g_i-2*m_x),
     alpha_z+1j*alpha_y*m_x*Q, -1j*alpha_y*Q/(2*alpha_z)*(alpha_y*
    g_r-2*m_x), -alpha_z+1j*alpha_y*m_x*Q],
                     [1j*n*g_i*Q/2, -n, 1j*n*g_r*Q/2, -n],
                     [n*alpha_z, 1j*n*g_i*Q/(2*alpha_z), -n*alpha_z
    , -1j*n*g_r*Q/(2*alpha_z)]])

#Creats a propagation matrix
def propagationmatrix(Q,M,alpha_y,alpha_z,n,lamda,d):
    m_x = M[0]
    m_y = M[1]
    m_z = M[2]
    U = np.exp(-1j*2*np.pi*n*alpha_z*d/lamda)
    g_i = m_z*alpha_z + alpha_y*m_y
    g_r = -m_z*alpha_z + alpha_y*m_y
    delta_i = np.pi*n*Q*d*g_i/(lamda*alpha_z)
    delta_r = np.pi*n*Q*d*g_r/(lamda*alpha_z)
    return np.array([[U*np.cos(delta_i), U*np.sin(delta_i), 0, 0],
                     [-U*np.sin(delta_i), U*np.cos(delta_i), 0, 0],
                     [0, 0, np.cos(delta_r)/U, -np.sin(delta_r)/U],
                     [0, 0, np.sin(delta_r)/U, np.cos(delta_r)/U]])



#Calculate the T matrix
#Variables: incident and final boundary matrix, a list of boundary
    matrices and propagation matrices for the layers
def Tmatrix(A_iinv, A_f, A, D):
    matrices = []
    matrices.append(A_iinv)
    if isinstance(A, list):
        for i in range(len(A)):
            matrices.append(A[i])
            matrices.append(D[i])
            matrices.append(inv(A[i]))
    else:
        matrices.append(A)
```

```
        matrices.append(D)
        matrices.append(inv(A))
    matrices.append(A_f)
    result = matrices[0]
    for i in range(1, len(matrices)):
        result = np.dot(result, matrices[i])
    return result

#Return Kerr rotation for s- and p-polarization
#Input: List of refractive index, magnetization strenght and direction, thicknessess. (total optical media)
#then also: wavelength of incident light, angle of incident.
#Returns Kerr_s, Kerr_p if Kerr=True
#Otherwise returns reflectance R (I_r = R*I_0) (for intensities in TMOKE): returns R_s, R_p
def MOKE(N, Q, M, d, wavelength, theta_i, Kerr=True):
    alpha_y = [np.sin(theta_i)]
    alpha_z = [np.sqrt(1-alpha_y[0]**2)]
    for i in range(len(N)-1):
        alpha_y.append(N[i]/N[i+1]*alpha_y[i])
        alpha_z.append(np.sqrt(1-alpha_y[i+1]**2))
    A_i = boundarymatrix(Q[0],M,alpha_y[0], alpha_z[0],N[0])
    A_iinv = inv(A_i)
    A_f = boundarymatrix(Q[-1],M,alpha_y[-1], alpha_z[-1],N[-1])
    A = []
    D = []
    for i in range(len(N)-2):
        A.append(boundarymatrix(Q[i+1], M, alpha_y[i+1], alpha_z[i+1], N[i+1]))
        D.append(propagationmatrix(Q[i+1], M, alpha_y[i+1], alpha_z[i+1], N[i+1], wavelength, d[i+1]))
    T = Tmatrix(A_iinv, A_f, A, D)
    G = np.array([[T[0,0], T[0,1]],
                  [T[1,0], T[1,1]]])
    I = np.array([[T[2,0], T[2,1]],
                  [T[3,0], T[3,1]]])
    R = I@inv(G)
    if Kerr == True:
        return R[1,0]/R[0,0], R[0,1]/R[1,1]
    else:
        return np.abs(R[0,0] + R[0,1])**2, np.abs(R[1,0] + R[1,1])**2

#Runs the MOKE function and vary two variables. It can vary M, d, wavelength or angle of incidence.
#Assumes:
# N, Q: 1D arrays.
# M: nx3, n = number of different directions. A = 1 if this is not varied (e.g np.array([[0,0,1]]))
# d: nxm, n = number of variations, m = number of slabs
#Returns the magniture of Kerr rotation for s and p
def runMOKE(N, Q, M, d, wavelength, theta_i, MOsignal = True, Kerr = True):
    if MOsignal == True:
        if len(M) > 1 and len(d) > 1:
            MOsignal_s = np.zeros((len(M),len(d)))
            MOsignal_p = np.zeros((len(M),len(d)))
```

```
98              for i in range(len(M)):
99                  for j in range(len(d)):
100                     Kerr_s, Kerr_p = MOKE(N[0], Q[0], M[i], d[j,:],
     wavelength, theta_i[0])
101                     MOsignal_s[i,j] = np.abs(Kerr_s)
102                     MOsignal_p[i,j] = np.abs(Kerr_p)
103             return MOsignal_s, MOsignal_p
104
105         elif len(M) > 1 and len(theta_i) > 1:
106             MOsignal_s = np.zeros((len(M),len(theta_i)))
107             MOsignal_p = np.zeros((len(M),len(theta_i)))
108             for i in range(len(M)):
109                 for j in range(len(theta_i)):
110                     Kerr_s, Kerr_p = MOKE(N[0], Q[0], M[i], d[0],
    wavelength, theta_i[j])
111                     MOsignal_s[i,j] = np.abs(Kerr_s)
112                     MOsignal_p[i,j] = np.abs(Kerr_p)
113             return MOsignal_s, MOsignal_p
114
115         elif len(M) > 1 and len(wavelength) > 1:
116             MOsignal_s = np.zeros((len(M),len(wavelength)))
117             MOsignal_p = np.zeros((len(M),len(wavelength)))
118             for i in range(len(M)):
119                 for j in range(len(wavelength)):
120                     Kerr_s, Kerr_p = MOKE(N[0], Q[0], M[i], d[0],
    wavelength[j], theta_i[0])
121                     MOsignal_s[i,j] = np.abs(Kerr_s)
122                     MOsignal_p[i,j] = np.abs(Kerr_p)
123             return MOsignal_s, MOsignal_p
124
125         elif len(theta_i) > 1 and len(wavelength) > 1:
126             MOsignal_s = np.zeros((len(theta_i),len(wavelength)))
127             MOsignal_p = np.zeros((len(theta_i),len(wavelength)))
128             for i in range(len(theta_i)):
129                 for j in range(len(wavelength)):
130                     Kerr_s, Kerr_p = MOKE(N[0], Q[0], M[0], d[0],
    wavelength[j], theta_i[i])
131                     MOsignal_s[i,j] = np.abs(Kerr_s)
132                     MOsignal_p[i,j] = np.abs(Kerr_p)
133             return MOsignal_s, MOsignal_p
134
135         else:
136             print('Hejsan')
137
138     elif MOsignal == False:
139         if len(M) > 1 and len(d) > 1:
140             AllKerr_s = np.zeros((len(M),len(d)), dtype='complex')
141             AllKerr_p = np.zeros((len(M),len(d)), dtype='complex')
142             for i in range(len(M)):
143                 for j in range(len(d)):
144                     Kerr_s, Kerr_p = MOKE(N[0], Q[0], M[i], d[j,:],
     wavelength, theta_i[0])
145                     AllKerr_s[i,j] = Kerr_s
146                     AllKerr_p[i,j] = Kerr_p
147             return AllKerr_s, AllKerr_p
148
149         elif len(M) > 1 and len(theta_i) > 1:
```

```
150             AllKerr_s = np.zeros((len(M),len(theta_i)), dtype='
    complex')
151             AllKerr_p = np.zeros((len(M),len(theta_i)), dtype='
    complex')
152             for i in range(len(M)):
153                 for j in range(len(theta_i)):
154                     Kerr_s, Kerr_p = MOKE(N[0], Q[0], M[i], d[0],
    wavelength, theta_i[j])
155                     AllKerr_s[i,j] = Kerr_s
156                     AllKerr_p[i,j] = Kerr_p
157             return AllKerr_s, AllKerr_p
158 
159         elif len(M) > 1 and len(wavelength) > 1:
160             AllKerr_s = np.zeros((len(M),len(wavelength)), dtype='
    complex')
161             AllKerr_p = np.zeros((len(M),len(wavelength)), dtype='
    complex')
162             for i in range(len(M)):
163                 for j in range(len(wavelength)):
164                     Kerr_s, Kerr_p = MOKE(N[0], Q[0], M[i], d[0],
    wavelength[j], theta_i[0])
165                     AllKerr_s[i,j] = Kerr_s
166                     AllKerr_p[i,j] = Kerr_p
167             return AllKerr_s, AllKerr_p
168 
169         elif len(theta_i) > 1 and len(wavelength) > 1:
170             AllKerr_s = np.zeros((len(theta_i),len(wavelength)),
    dtype='complex')
171             AllKerr_p = np.zeros((len(theta_i),len(wavelength)),
    dtype='complex')
172             for i in range(len(theta_i)):
173                 for j in range(len(wavelength)):
174                     Kerr_s, Kerr_p = MOKE(N[0], Q[0], M[0], d[0],
    wavelength[j], theta_i[i])
175                     AllKerr_s[i,j] = Kerr_s
176                     AllKerr_p[i,j] = Kerr_p
177             return AllKerr_s, AllKerr_p
178 
179         #Q depends on wavelength, so len(Q) = len(wavelength)
180         elif len(Q) > 1:
181             if Kerr == True:
182                 print('not working')
183                 AllKerr_s = np.zeros(len(Q), dtype='complex')
184                 AllKerr_p = np.zeros(len(Q), dtype='complex')
185                 for i in range(len(Q)):
186                     Kerr_s, Kerr_p = MOKE(N[i], Q[i], M[0], d[0],
    wavelength[i], theta_i[0], Kerr)
187                     AllKerr_s[i] = Kerr_s
188                     AllKerr_p[i] = Kerr_p
189                 return AllKerr_s, AllKerr_p
190 
191             elif Kerr == False:
192                 print('working')
193                 AllKerr_s = np.zeros(len(Q))
194                 AllKerr_p = np.zeros(len(Q))
195                 for i in range(len(Q)):
```

```
                    Kerr_s, Kerr_p = MOKE(N[i], Q[i], M[0], d[0],
    wavelength[i], theta_i[0], Kerr)
                    AllKerr_s[i] = Kerr_s
                    AllKerr_p[i] = Kerr_p
                return AllKerr_s, AllKerr_p

        else:
            print('Hejsan')

    else:
        print('Something is wrong')
```

Code that runs the simulation above.

```
import numpy as np
import improved_general as ig
from get_data import load_data

#Inputs:
#    element(type=tuple): ('element', d), where element = 'Ni', 'Fe'
     or 'Co', and d = thickness
#    coating(type=tuple): (N,d) - refractive index and thickness (in
     nm), put = None if no coating
#    substrate(type=complex): N - refractive index, put = None if no
     substrate
#    AoI(type=numpy array): np.array([]) - array of angle of
    incidence in radians
#    MOKEtype(type=str): 'L', 'T' or 'P', for LMOKE, TMOKE or PMOKE
#    measurement(type=str): 'K', 'S', 'A', for Kerr rotation, Signal
    (abs(Kerr rot)), or Asymmetry measurement
#    filename(type=str): 'filename' - filename for the data to be
    stored (it will be stored as np arrays)
def runSim(element, coating, substrate, AoI, MOKEtype, measurement,
     filename):

    epsilonRe, epsilonIm, energies, N, Q = load_data(f'{element[0]}
    ')

    #Wavelength and d(thickness) need to have same unit. Only
    things with units!
    #From eV to meter
    wavelength = 1239.84193/energies #nm

    #Experimental setup
    N_air = np.zeros(len(N)) + 1
    Q_air = np.zeros(len(N))

    if coating is None and substrate is None:
        Ns = np.vstack((N_air, N)).T
        Qs = np.vstack((Q_air, Q)).T
        ds = np.array([[0,0]])

    elif coating is None and substrate is not None:
        N_substrate = np.zeros(len(N)) + substrate
        Q_substrate = np.zeros(len(N))
        Ns = np.vstack((N_air, N, N_substrate)).T
        Qs = np.vstack((Q_air, Q, Q_substrate)).T
        ds = np.array([[0, element[1], 0]])
```

```
36
37      elif coating is not None and substrate is None:
38          N_coating = np.zeros(len(N)) + coating[0]
39          Q_coating = np.zeros(len(N))
40          Ns = np.vstack((N_air, N_coating, N)).T
41          Qs = np.vstack((Q_air, Q_coating, Q)).T
42          ds = np.array([[0, coating[1], 0]])
43
44      else:
45          N_coating = np.zeros(len(N)) + coating[0]
46          Q_coating = np.zeros(len(N))
47          N_substrate = np.zeros(len(N)) + substrate
48          Q_substrate = np.zeros(len(N))
49          Ns = np.vstack((N_air, N_coating, N, N_substrate)).T
50          Qs = np.vstack((Q_air, Q_coating, Q, Q_substrate)).T
51          ds = np.array([[0, coating[1], element[1], 0]])
52
53      #Magnetizaiton diraction
54      if MOKEtype == 'L':
55          M = np.array([[0,1,0]])
56      elif MOKEtype == 'T':
57          M = np.array([[1,0,0]])
58      elif MOKEtype == 'P':
59          M = np.array([[0,0,1]])
60      else:
61          print('Specify MOKE type')
62
63      thetas = AoI
64      if measurement == 'A':
65          data = np.empty((0,4,energies.size))
66
67          for theta in thetas:
68              theta = np.array([theta])
69              I_spos, I_ppos = ig.runMOKE(Ns, Qs, M, ds, wavelength,
    theta, False, False)
70              I_sneg, I_pneg = ig.runMOKE(Ns, Qs, -M, ds, wavelength,
     theta, False, False)
71              I_all = np.concatenate((I_spos.reshape(1,-1), I_ppos.
    reshape(1,-1), I_sneg.reshape(1,-1), I_pneg.reshape(1,-1)),axis
    =0)
72              data = np.concatenate((data, I_all.reshape(1,4,-1)),
    axis=0)
73
74          np.save(f'Data/{filename}_Asymmetry_data.npy', data)
75          np.save(f'Data/{filename}_Asymmetry_energies.npy', energies
    )
76          np.save(f'Data/{filename}_Asymmetry_thetas.npy', thetas)
77      else:
78          print('Specify what kind of measurement you want. Currently
     only A for asymmetry works.')
```